

Supporting Information: DNA Interstrand Cross-link Formation by the 1,4-Dioxobutane Abasic Lesion.

Lirui Guan and Marc M. Greenberg*

Department of Chemistry, Johns Hopkins University, 3400 N. Charles St., Baltimore, MD 21218

mgreenberg@jhu.edu

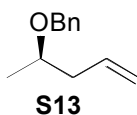
Reference 34: Mueller, R.; Yang, J.; Duan, C.; Pop, E.; Zhang, L. H.; Huang, T.-B.; Denisenko, A.; Denisko, O. V.; Oniciu, D. C.; Bisgaier, C. L.; Pape, M. E.; Freiman, C. D.; Goetz, B.; Cramer, C. T.; Hopson, K. L.; Dasseux, J.-L. *J. Med. Chem.* **2004**, *47*, 5183–5197.

Contents:

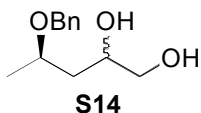
1. General Methods (S2)
2. Experimental Procedures. (S2-S12)
3. **Supporting Information Figure 1.** ^1H NMR spectrum of **S13**. (S13)
4. **Supporting Information Figure 2.** ^{13}C NMR spectrum of **S13**. (S14)
5. **Supporting Information Figure 3.** ^1H NMR spectrum of **S14**. (S15)
6. **Supporting Information Figure 4.** ^{13}C NMR spectrum of **S14**. (S16)
7. **Supporting Information Figure 5.** ^1H NMR spectrum of **S15**. (S17)
8. **Supporting Information Figure 6.** ^{13}C NMR spectrum of **S15**. (S18)
9. **Supporting Information Figure 7.** ^1H NMR spectrum of **S16**. (S19)
10. **Supporting Information Figure 8.** ^{13}C NMR spectrum of **S16**. (S20)
11. **Supporting Information Figure 9.** ^1H NMR spectrum of **9**. (S21)
12. **Supporting Information Figure 10.** ^{31}P NMR spectrum of **9**. (S22)
13. **Supporting Information Figure 11.** ^1H NMR spectrum of **S17**. (S23)
14. **Supporting Information Figure 12.** ^{13}C NMR spectrum of **S17**. (S24)
15. **Supporting Information Figure 13.** ^1H NMR spectrum of **S18**. (S25)
16. **Supporting Information Figure 14.** ^{13}C NMR spectrum of **S18**. (S26)
17. **Supporting Information Figure 15.** ^1H NMR spectrum of **10**. (S27)
18. **Supporting Information Figure 16.** ^{31}P NMR spectrum of **10**. (S28)
19. **Supporting Information Figure 17.** ^1H NMR spectrum of **5**. (S29)
20. **Supporting Information Figure 18.** ^{13}C NMR spectrum of **5**. (S30)
21. **Supporting Information Figure 19.** ESI-MS/MS of **4**. (S31)
22. **Supporting Information Figure 20.** ESI-MS of oligonucleotide containing the DOB precursor (local sequence: 5'-XAC). (S32)
23. **Supporting Information Figure 21.** ESI-MS of oligonucleotide containing the DOB precursor (local sequence: 5'-XTC). (S33)
24. **Supporting Information Figure 22.** ESI-MS of oligonucleotide containing the DOB precursor (local sequence: 5'-XGC). (S34)
25. **Supporting Information Figure 23.** ESI-MS of oligonucleotide containing the DOB precursor (local sequence: 5'-XCC). (S35)
26. **Supporting Information Figure 24.** ESI-MS of oligonucleotide containing the precursor of **7** (local sequence: 5'-XTC). (S36)

27. **Supporting Information Figure 25.** ESI-MS of oligonucleotide containing the precursor of **8** (local sequence: 5'-XTC). (S37)
28. **Supporting Information Figure 26.** ESI-MS of the ICL (**3k**) obtained from the ternary complex **2k**. (S38)
29. **Supporting Information Figure 27.** Hydroxyl radical cleavage of **3a**. (S39)
30. **Supporting Information Figure 28.** Hydroxyl radical cleavage of **3c**. (S40)
31. **Supporting Information Figure 29.** Hydroxyl radical cleavage of **3i**. (S41)
32. **Supporting Information Figure 30.** Hydroxyl radical cleavage of **3j**. (S42)
33. **Supporting Information Figure 31.** Hydroxyl radical cleavage of **3k**. (S43)
34. **Supporting Information Figure 32.** Hydroxyl radical cleavage of **3l**. (S44)
35. **Supporting Information Figure 33.** Hydroxyl radical cleavage of **3m**. (S45)
36. **Supporting Information Figure 34.** Hydroxyl radical cleavage of **3p**. (S46)
37. **Supporting Information Figure 35.** Plot of ICL **3i** decomposition as a function of time. (S47)
38. **Supporting Information Figure 36.** Kinetic plot of monomer 1,4-butanedial adduct decomposition. (S48)

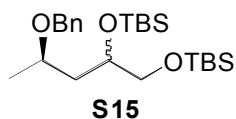
General Methods. Oligonucleotides were synthesized on an Applied Biosystems Incorporated 394 oligonucleotide synthesizer. Oligonucleotide synthesis reagents were purchased from Glen Research (Sterling, VA). All chemicals were purchased from either Sigma-Aldrich or Acros and were used without further purification. ESI-MS analysis was carried out on a LCQ-Deca Ion Trap. All Oligonucleotides were precipitated from 1.25 M ammonium acetate (pH 5.6) prior to analysis. T4 polynucleotide kinase and terminal deoxytransferase were obtained from New England Biolabs. γ - ^{32}P -ATP and α - ^{32}P -cordycepin 5'-triphosphate were purchased from Perkin Elmer. C18-Sep-Pak cartridges were obtained from Waters. Quantification of radiolabeled oligonucleotides was carried out using a Molecular Dynamics Phosphorimager 840 equipped with ImageQuant Version 5.1 software. All photolyses of oligonucleotides were carried out in clear eppendorf tubes in a Rayonet photoreactor (RPR-100) fitted with 16 lamps having an output maximum at 350 nm.



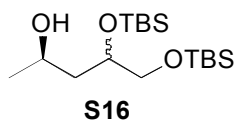
Compound S13. To a solution of **11**¹ (1.0 g, 0.012 mol) in THF (60 mL) was added NaH (720 mg, 0.018 mol, 60% dispersion in oil). The mixture was stirred at 25 °C for 1 h. Benzylbromide (2.86 mL, 0.024 mol) was added dropwise and the mixture was stirred at 25 °C overnight. The mixture was quenched with saturated NH₄Cl (60 mL) and extracted with diethyl ether (3 x 60 mL). The combined organic layers were washed with brine, dried over Na₂SO₄, and concentrated under reduced pressure. The residue was purified by column chromatography (1% ethyl acetate in hexanes to 5% ethyl acetate in hexanes) to give **S13** (961 mg, 93%). ¹H NMR (CDCl₃) δ 1.21-1.23 (2s, 3H), 2.27 (m, 1H), 2.39 (m, 1H), 3.60 (m, 1H), 4.48-4.60 (m, 2H), 5.06-5.13 (m, 2H), 5.85 (m, 1H), 7.27-7.36 (m, 5H); ¹³C NMR (CDCl₃) δ 19.7, 41.1, 70.6, 74.7, 117.1, 127.6, 127.8, 128.5, 135.3, 139.2; IR (neat) 3028, 2926, 2857, 1727, 1508, 1496, 1454, 1374, 1229, 1092, 913, 735, 698 cm⁻¹.



Compound S14. To a solution of **S13** (883 mg, 5 mmol) and NMO (878 mg, 6.5 mmol) in acetone/H₂O (10 : 1, 33 mL) was added OsO₄ (63.5 mg, 0.25 mmol). The mixture was stirred at 25 °C for 1 h. The solvent was removed under reduced pressure. The residue was purified by column chromatography (75% ethyl acetate in hexanes) to give **S14** (796 mg, 76%). ¹H NMR (CDCl₃) δ 1.28 (m, 3H), 1.58 (m, 1H), 1.79 (m, 1H), 2.14-2.23 (m, 1H), 3.04 and 3.84 (m, 1H), 3.46 (m, 1H), 3.60 (m, 1H), 3.87-4.03 (m, 2H), 4.42-4.47 (m, 1H), 4.63-4.70 (m, 1H), 7.27-7.37 (m, 5H); ¹³C NMR (CDCl₃) δ 19.5, 19.9, 39.3, 40.1, 66.9, 67.1, 69.3, 70.6, 70.8, 71.9, 72.7, 75.6, 128.0, 128.1, 128.7, 128.8, 138.1, 138.5; IR (neat) 3389, 3031, 2968, 2931, 2872, 1496, 1454, 1376, 1342, 1207, 1145, 1060, 1027, 736, 698 cm⁻¹; FAB-HRMS (M⁺ + H) for C₁₂H₁₉O₃: calcd 211.1329, found 211.1335.



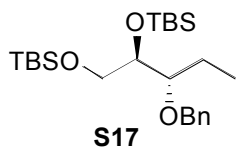
Compound S15. To a solution of compound **S14** (500 mg, 2.38 mmol) in dry DMF (12 mL) was added imidazole (1.94 g, 28.6 mmol) and TBDMSCl (2.14 g, 14.3 mmol). After stirring at 25 °C for 8 h, the reaction mixture was diluted with diethyl ether and washed with saturated NH₄Cl and brine. The organic phase was dried over Na₂SO₄ and the solvent was removed under reduced pressure. The residue was purified by column chromatography (5% ethyl acetate in hexanes) to give **S15** (712 mg, 68%). ¹H NMR (CDCl₃) δ 0.04 (m, 12H), 0.89 (m, 18H), 1.24 (m, 3H), 1.42-1.70 (m, 1H), 1.79-1.90 (m, 1H), 3.46-3.56 (m, 2H), 3.68-3.94 (m, 2H), 4.41-4.62 (m, 2H), 4.42-4.47 (m, 1H), 7.27-7.35 (m, 5H); ¹³C NMR (CDCl₃) δ -5.1, -4.6, -4.5, -3.9, -3.8, 18.3, 18.4, 18.6, 18.7, 20.1, 20.5, 26.1, 26.20, 26.21, 26.24, 41.8, 42.8, 67.9, 68.3, 70.2, 70.4, 70.8, 71.1, 72.2, 127.47, 127.54, 127.6, 127.8, 128.5, 139.3, 139.4; IR (neat) 2957, 2858, 1472, 1374, 1255, 1107, 836, 776, 733, 696 cm⁻¹; FAB-HRMS (M⁺ + H) for C₂₄H₄₇O₃Si₂: calcd 439.3064, found 439.3064.



Compound S16. A solution of compound **S15** (688 mg, 1.57 mmol) and Pd(OH)₂/C (688 mg) in ethyl acetate (5 mL) was stirred at 25 °C under H₂ (50 psi) overnight. The mixture was passed through a pad of celite, which was then washed with ethyl acetate. The solvent was removed under reduced pressure and the residue was purified by column chromatography (25% ethyl acetate in hexanes) to give **S16** (442 mg, 81%). ¹H NMR (CDCl₃) δ 0.10 (m, 12H), 0.9 (m, 18H), 1.17-1.20 (m, 3H), 1.54-1.80 (m, 2H), 3.33-3.66 (m, 3H), 3.88-4.10 (m, 2H); ¹³C NMR (CDCl₃) δ -5.25, -5.20, -5.16, -4.8, -4.6, -4.4, -3.9, 18.2, 18.5, 18.6, 23.7, 24.1, 26.0, 26.1, 42.3,

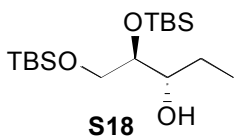
43.7, 64.8, 66.2, 66.3, 67.9, 72.5, 73.2; IR (neat) 3450, 2956, 2930, 2858, 1472, 1361, 1255, 1107, 939, 835, 777, 669 cm^{-1} ; FAB-HRMS ($\text{M}^+ + \text{H}$) for $\text{C}_{17}\text{H}_{41}\text{O}_3\text{Si}_2$: calcd 349.2594, found 349.2589.

Phosphoramidite 9. To solution of **S16** (230 mg, 0.66 mmol) in CH_2Cl_2 (3 mL) was added DIPEA (0.5 mL, 2.9 mmol) and 2-cyanoethyl *N,N*-diisopropylchlorophosphoramidite (234.5 mg, 221 μL , 0.99 mmol). The mixture was stirred at 25 $^\circ\text{C}$ overnight under argon. The mixture was diluted with ethyl acetate, washed with saturated NaHCO_3 , water, followed by brine. The organic phase was dried over Na_2SO_4 and concentrated. The residue was purified by column chromatography (5 % ethyl acetate in hexanes) to give **9** (243 mg, 67%). ^1H NMR (CDCl_3) δ 0.04-0.12 (m, 12H), 0.90 (m, 18H), 1.17-1.20 (m, 3H), 1.47-1.50 (m, 1H), 1.81-1.89 (m, 1H), 2.63 (t, 2H, $J = 6.4$ Hz), 3.36-3.85 (m, 7H), 4.16 (m, 1H); ^{31}P NMR (CDCl_3) δ 145.8, 145.85, 145.90, 146.8, 146.9; FAB-HRMS ($\text{M}^+ + \text{Na}$) for $\text{C}_{26}\text{H}_{57}\text{N}_2\text{O}_4\text{NaSi}_2\text{P}$: calcd 571.3492, found 571.3501.



Compound S17. To a solution of compound **12**^{2,3} (409 mg, 1.95 mmol) in dry DMF (10 mL) was added imidazole (1.6 g, 23.4 mmol) and TBDMSCl (1.76 g, 11.7 mmol). After stirring at 25 $^\circ\text{C}$ overnight, the reaction mixture was diluted with diethyl ether and washed with saturated NH_4Cl , followed by brine. The organic phase was dried over Na_2SO_4 and the solvent was removed under reduced pressure. The residue was purified by column chromatography (10% ethyl acetate in hexanes) to give **S17** (665 mg, 78%). ^1H NMR (CDCl_3) δ 0.06-0.09 (m, 12H), 0.90 (m, 18H), 0.95 (t, 3H, $J = 7.6$ Hz), 1.59 (m, 2H), 3.42 (m, 1H), 3.65 (m, 2H), 3.80 (m, 1H), 4.50-4.70 (dd, 2H, $J = 69.2, 11.6$ Hz), 7.27-7.36 (m, 5H); ^{13}C NMR (CDCl_3) δ -5.2, -5.1, -4.6, -

4.1, 10.5, 18.4, 18.6, 23.3, 26.1, 26.2, 65.1, 72.7, 75.2, 82.3, 127.6, 128.1, 128.4, 139.3; IR (neat) 2957, 2930, 2858, 1463, 1361, 1255, 1105, 835, 777, 732, 696 cm^{-1} ; FAB-HRMS ($\text{M}^+ + \text{H}$) for $\text{C}_{24}\text{H}_{47}\text{O}_3\text{Si}_2$: calcd 439.3064, found 439.3063.



Compound S18. A solution of **S17** (600 mg, 1.37 mmol) and $\text{Pd}(\text{OH})_2/\text{C}$ (300 mg) in ethyl acetate (10 mL) was stirred at 25 °C under H_2 (50 psi) overnight. The mixture was passed through a pad of celite, which was then washed with ethyl acetate. The solvent was removed under reduced pressure and the residue was purified by column chromatography (5% ethyl acetate in hexanes) to give **S18** (396 mg, 83%). ^1H NMR (CDCl_3) δ 0.08-0.09 (m, 12H), 0.90 (m, 18H), 1.00 (t, 3H, $J = 7.6$ Hz), 1.38-1.62 (m, 2H), 2.91 (m, 1H), 3.57-3.67 (m, 4H); ^{13}C NMR (CDCl_3) δ -5.34, -5.26, -4.6, -4.1, 10.5, 18.3, 18.5, 25.6, 26.0, 26.1, 66.0, 74.8; IR (neat) 3451, 2958, 2931, 2859, 1472, 1390, 1362, 1256, 1098, 1006, 976, 939, 836, 777, 667 cm^{-1} ; FAB-HRMS ($\text{M}^+ + \text{H}$) for $\text{C}_{17}\text{H}_{41}\text{O}_3\text{Si}_2$: calcd 349.2594, found 349.2596.

Phosphoramidite 10. To solution of **S18** (170 mg, 0.49 mmol) in CH_2Cl_2 (2 mL) was added DIPEA (371 mg, 0.5 mL, 2.9 mmol) and 2-cyanoethyl *N,N*-diisopropylchlorophosphoramidite (177 mg, 167 μL , 0.75 mmol). The mixture was stirred at 25 °C overnight under argon. The mixture was diluted with ethyl acetate, washed with saturated NaHCO_3 , water, and then brine. The organic phase was dried over Na_2SO_4 and concentrated. The residue was purified by column chromatography (5 % ethyl acetate in hexanes) to give **10** (162 mg, 61%). ^1H NMR (CDCl_3) δ 0.05-0.11 (m, 12H), 0.89-0.90 (m, 18H), 0.91-1.00 (m, 3H), 1.18-1.20 (m, 12H), 1.58-1.63 (m, 2H), 2.63 (t, 2H, $J = 6.4$ Hz), 3.53 (m, 1H), 3.63 (m, 3H), 3.78 (m, 2H), 3.85 (m, 2H); ^{31}P NMR

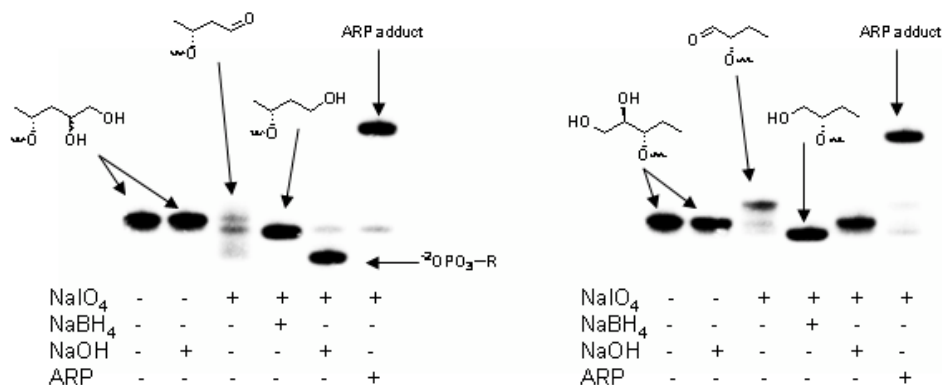
(CDCl₃) δ 147.6, 150.0; FAB-HRMS ($M^+ + H$) for C₂₆H₅₈N₂O₄Si₂P: calcd 549.3673, found 549.3680.

Synthesis of Oligonucleotides Containing Lesion Precursors. Standard synthesis cycles (25 s coupling, 5 s capping with acetic anhydride, 15 s oxidation with 1 M *t*-butyl hydroperoxide in THF, 95 s detritylation with 3% TCA in methylene chloride) were used prior to the incorporation of the lesion precursor. The phosphoramidite of the lesion was incorporated with 5 min (for DOB containing oligonucleotides) or 30 min (for DOB model compound containing oligonucleotides) coupling, 25 s capping, 40 s oxidation using the same synthesis reagents. After AMA (conc. aq. ammonia : methylamine v/v 1:1) deprotection (55 °C, 10 min), the oligonucleotides were purified by 20% denaturing PAGE.

General Procedure for ICL Formation in DOB Containing Ternary Complexes. The ternary complex containing 3'-³²P-labeled DOB oligonucleotide was prepared using the previously reported method.⁴ The freshly hybridized ternary complex (2 μ M) in PBS buffer (100 mM NaCl and 10 mM potassium phosphate, pH 7.2) was photolyzed for 60 min at 25 °C. The solution was then diluted to 1 μ M with PBS buffer (100 mM NaCl and 10 mM potassium phosphate, pH 7.2). The reaction (40 μ L) was incubated at 37 °C for 24 h. When the reaction was complete, an aliquot (1 μ L) of the reaction solution was mixed with formamide loading buffer (5 μ L) and the cross-link was resolved using 20% denaturing PAGE.

General Procedure for ICL Formation in DOB Model Compound (7 or 8) Containing Ternary Complexes. The ternary complex was prepared in the same manner described above for DOB containing ternary complexes. The freshly hybridized ternary complex (1 μ M) in PBS buffer (100 mM NaCl and 10 mM potassium phosphate, pH 7.2) was incubated with NaIO₄ (2.5 mM) at 37 °C for 30 min in a total volume of 80 μ L. An aliquot (40 μ L) was removed. One part

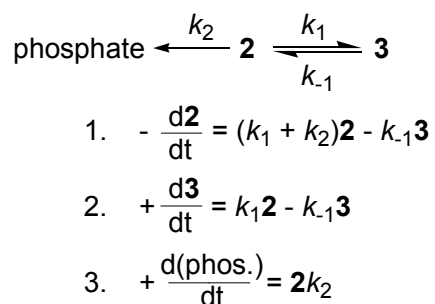
(10 μL) was treated with NaOH (10 μL , 0.2 M) at 37 $^{\circ}\text{C}$ for 30 min. One part (10 μL) was treated with NaBH₄ (10 μL , 500 mM) at 25 $^{\circ}\text{C}$ for 1 h. One part (10 μL) was treated with ARP (aldehyde reactive probe, 10 μL , 10 mM) at 25 $^{\circ}\text{C}$ for 1 h. The formation of **7** and **8** were resolved using 20% denaturing PAGE.



Following oxidation by NaIO₄, the solution was incubated at 37 $^{\circ}\text{C}$ for 24 h. An aliquot (1 μL) was removed and mixed with formamide loading buffer (5 μL) and the cross-link was resolved using 20% denaturing PAGE.

Kinetic Study of DOB Containing Ternary Complexes. The freshly hybridized ternary complex **2i** (2 μM) in PBS buffer (100 mM NaCl and 10 mM potassium phosphate, pH 7.2) was photolyzed for 60 min at 25 $^{\circ}\text{C}$. The solution was then diluted to 1 μM with PBS buffer (100 mM NaCl and 10 mM potassium phosphate, pH 7.2). The reaction (40 μL) was incubated at 37 $^{\circ}\text{C}$ for 27 h. Aliquots (2 μL) were removed at the indicated times. From each aliquot one part (1 μL) was directly mixed with formamide loading buffer (5 μL) and stored at -80 $^{\circ}\text{C}$. Another part (1 μL) was treated with NaBH₄ (0.5 μL , 500 mM) and incubated at 25 $^{\circ}\text{C}$ for 30 min. The solution was then mixed with formamide loading buffer (5 μL) and stored at -80 $^{\circ}\text{C}$. The cross-link and 3'-phosphate elimination product were resolved using 20% denaturing PAGE and quantified using the phosphorimager. The percentage of ICL (**3**), remaining DOB (**2**) and 3'-

phosphate at indicated times were fit using the equations below to determine the appropriate rate constants. Fitting was done iteratively using Origin 6.1.



Determination of ICL Location Using the Hydroxyl Radical Cleavage Reaction. The ternary complexes containing a DOB containing strand, a flanking strand and a 5'-labeled complementary strand were incubated at 37 °C for 24 h in PBS. The interstrand cross-link product was purified by 20% PAGE. The bands corresponding to the cross-link products were carefully excised from the gel, crushed, and eluted in 500 μL of water for 1 h at room temperature with constant vortexing. The solution was filtered using a 10 mL Polyprep column (Biorad) and desalted using a C₁₈-Sep-Pak column (100 mg). After concentration, a portion of the DNA (~30,000 cpm) was dissolved in 8 μL of water and mixed with 10 μL of the 2 \times oxidation buffer (20 mM NaCl, 20 mM sodium phosphate, pH 7.2, 2 mM sodium ascorbate, and 1 mM hydrogen peroxide). The reaction was initiated by adding 2 μL of the Fe•EDTA solution (1 mM EDTA and 0.5 mM Fe(NH₄)₂(SO₄)₂•6H₂O), and the reaction was allowed to proceed for no longer than 3 min. The reaction was quenched with 10 μL of 100 mM thiourea and concentrated. The DNA was resuspended in formamide loading buffer (5 μL) and separated by 20% PAGE.

Determination of Reversible ICL Formation. To determine the rate of decomposition and the decomposed product of **3i**, the cross-link was isolated from **2i** in the same manner described above for the hydroxyl-radical cleavage reactions. The isolated ICL material was dissolved in

PBS (100 mM NaCl and 10 mM potassium phosphate, pH 7.2) and divided into two portions. One portion was then incubated for 9 h at 37 °C. Aliquots (1 µL) were removed at the indicated time, directly mixed with formamide loading buffer (5 µL) and stored at -80 °C. Another portion was incubated in Tris•HCl (50 mM, pH 7.2) for 9 h at 37 °C. Aliquots (1 µL) were removed at the indicated time, treated with NaBH₄ (0.5 µL, 500 mM) and incubated at 25 °C for 30 min. The solution was then mixed with formamide loading buffer (5 µL) and stored at -80 °C. The remaining cross-link and the DOB/Tris adduct were resolved using 20% denaturing PAGE.

Compound 5. To a solution of 2'-deoxyadenosine (12.6 mg, 0.05 mmol) in potassium phosphate buffer (50 mM, pH 7.2) was added fresh prepared 1,4-butanedia⁵ (43 mg, 0.5 mmol). The resulting mixture was incubated at 37 °C for 24 h. The reaction solution was eluted from HPLC (Delta Pak C18 15 µm semi-prep column, 300 mm × 7.8 mm, Waters) with a linear gradient starting with 100% solvent A (H₂O) to 95% A and 5% B (acetonitrile) over 30 min with a flow rate of 3 mL/min. Adduct **4** eluted at 16.3 min. Upon concentration, **4** partially decomposed to dA. ESI-MS (M⁺) for C₁₄H₁₉N₅O₅: calcd 337.33, found 337.61.

The residue (6.5 mg) containing **4** and decomposition products was suspended in water (2 mL) and the solution was adjusted to pH = 5.0 by adding glacial acetic acid (0.5 µL). NaCNBH₃ (6.3 mg, 0.1 mmol) was added to the solution and the mixture was incubated at 25 °C for 6 h. The solvent was removed under vacuum and the residue was purified by column chromatography (5 % MeOH in CH₂Cl₂). The product (3.1 mg, 0.01 mmol) obtained was dissolved in dry DMF (0.2 mL). To this solution was added imidazole (5.4 mg, 0.08 mmol) and TBDMSCl (6 mg, 0.04 mmol). After stirring at 25 °C overnight, the reaction mixture was diluted with diethyl ether and washed with saturated NH₄Cl, followed by brine. The organic phase was dried over Na₂SO₄ and the solvent was removed under reduced pressure. The residue was

purified by column chromatography (25% ethyl acetate in hexanes) to give **5** (4.3 mg, 80%). ¹H NMR (CDCl₃) δ 0.08-0.10 (2s, 12H), 0.91 (2s, 18H), 2.03 (br s, 4H), 2.40 (m, 1H), 2.61 (m, 1H), 3.75-3.83 (m, 2H), 3.76 (br s, 2H), 4.01 (m, 1H), 4.15 (br s, 2H), 4.60 (m, 1H), 6.46 (t, 1H, *J* = 6.4 Hz), 7.97 (s, 1H), 8.35 (s, 1H); ¹³C NMR (CDCl₃) δ -5.3, -5.1, -4.6, -4.5, 18.2, 18.6, 26.0, 26.2, 41.2, 63.1, 72.4, 84.3, 88.1, 120.8, 137.4, 149.9, 152.5. FAB-HRMS (*M*⁺ + H) for C₂₆H₄₈N₅O₃Si₂ calcd. 534.3296 found 534.3286. These data are identical to the published results.⁶

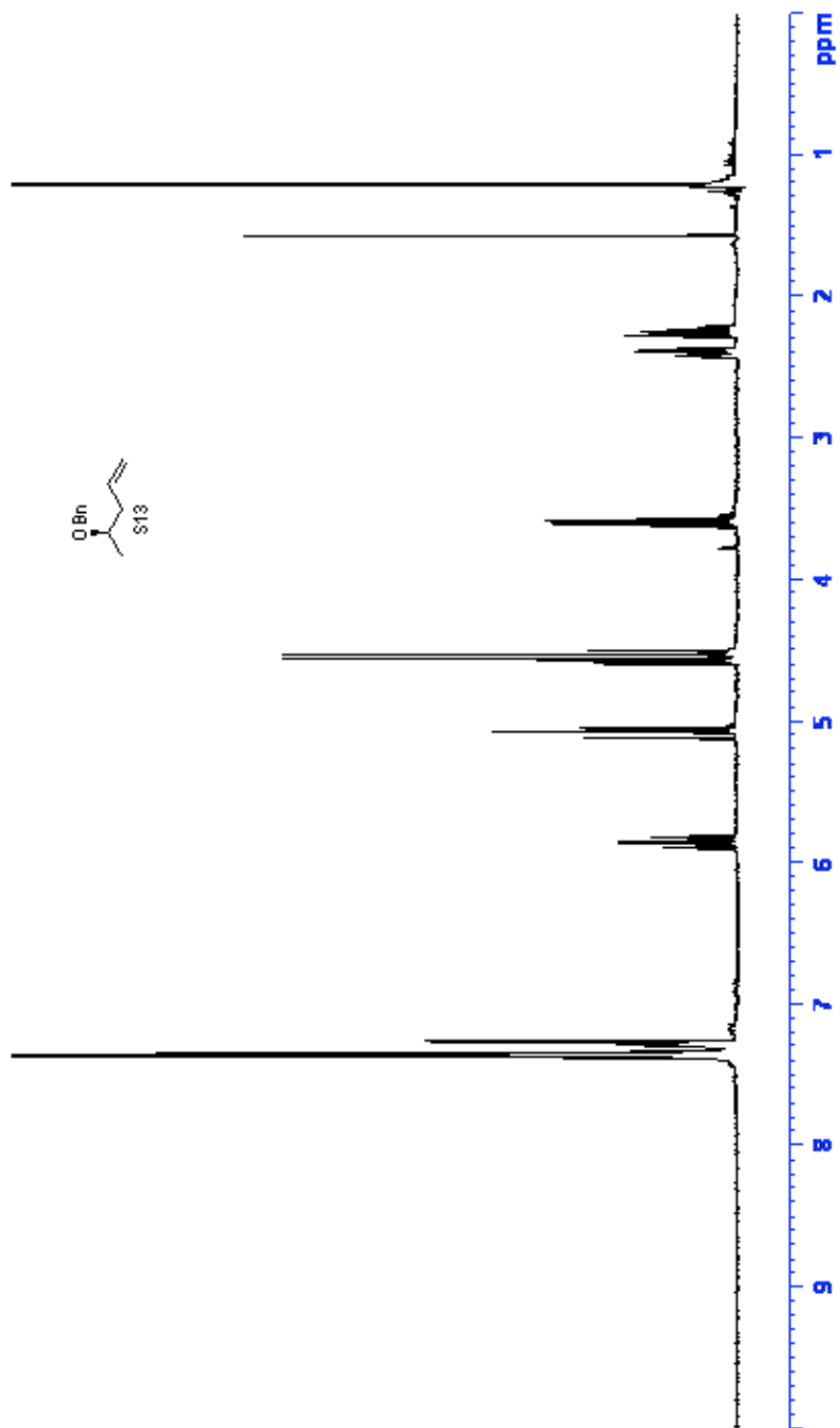
General Procedure for the Determination of the Rate Constant for Monomer Adduct Formation. A solution (1 mL) of 2'-deoxyribonucleoside (dA, dG or dC, 1 mM), 1,4-butanediol (50 mM) and thymine (1 mM, as internal standard) was incubated at 25 °C for 24 h. Aliquots (20 μL) were removed at the indicated times. Adduct formation was analyzed using HPLC (Microsorb-MV C₁₈ 5 μm column, 250 × 4.6 mm). Products were eluted with a linear gradient starting from 95% solvent A (H₂O) and 5% solvent B (acetonitrile) to 80% A and 20% B over 30 min with a flow rate of 1 mL/min. Retention times (min): dC adduct, 12.9; dA adduct, 14.9; dG adduct, 16.8, thymine, 8.1.

General Procedure for the Determination of the Rate Constant for Monomer Adduct Decomposition. The monomer adduct was isolated in the same manner described above for **4** during the preparation of compound **5**. The adduct and thymine (1 mM, as internal standard) were incubated at 25 °C for 24 h. Aliquots (20 μL) were removed at the indicated times. The disappearance of adduct was analyzed for using the same HPLC method described above for the formation of monomer adduct.

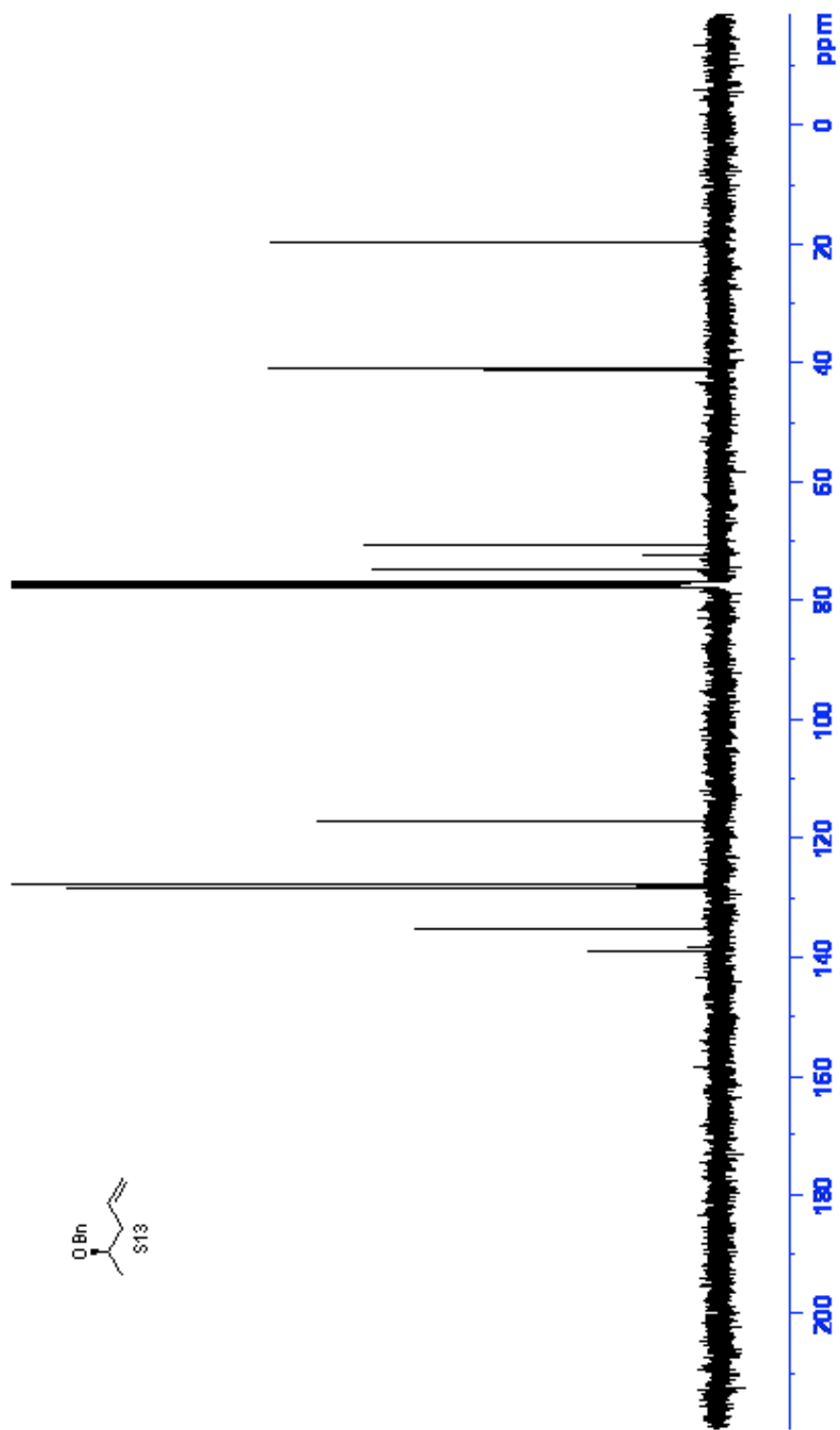
Preparation of ICL 3k for ESI-MS. Ternary complex **2k** (60 nmol) was photolyzed for 1 h in 1.5 mL of PBS (100 mM NaCl, 10 mM sodium phosphate, pH 7.2) before being diluted to 9

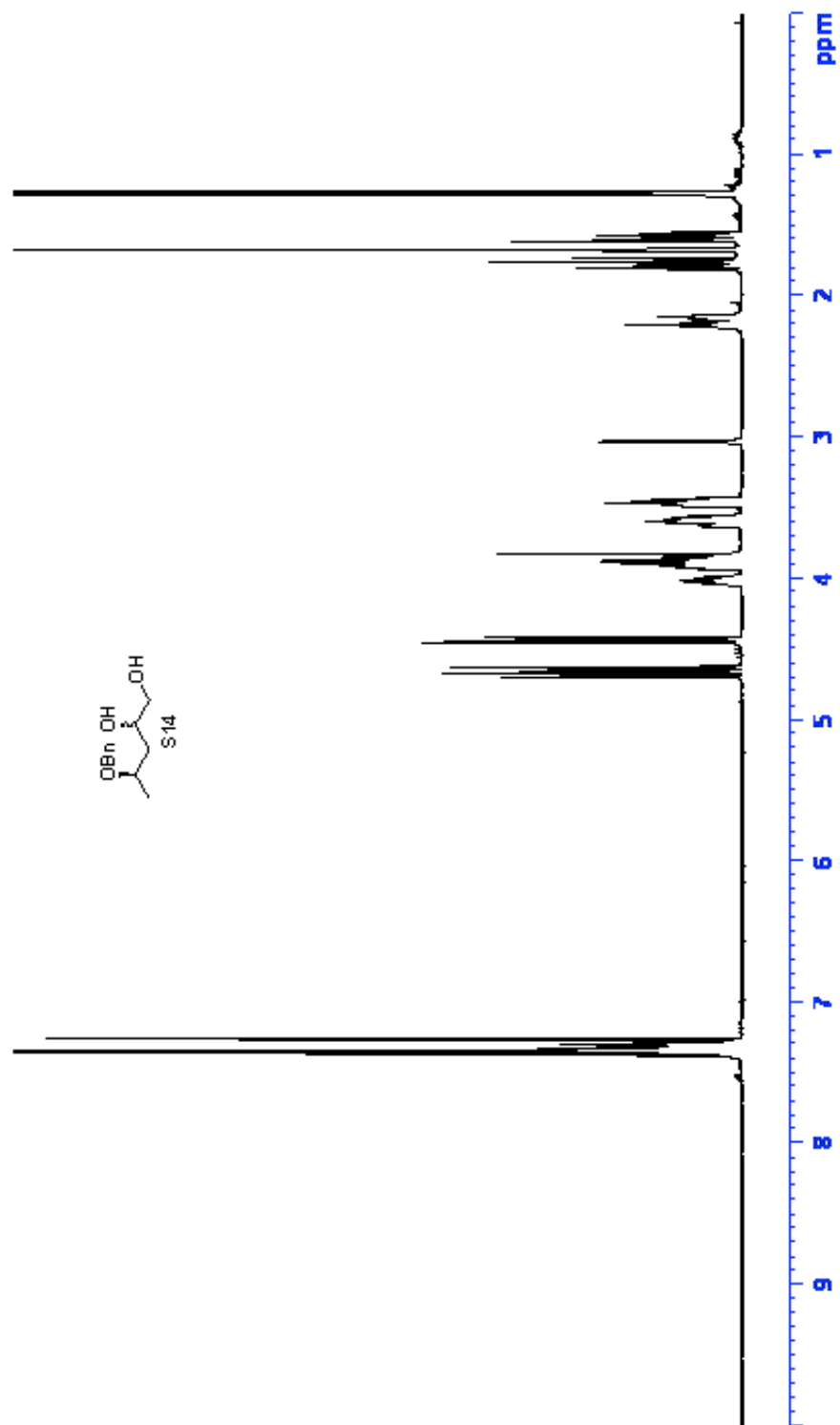
mL in PBS. The reaction was incubated at 37 °C for 24 h and concentrated. The material was purified using 20% denaturing PAGE and the band corresponding to ICL was cut from the gel, crushed, and eluted at 25 °C in 10 mL water for 1 h. The material was desalted and concentrated using a C₁₈-Sep-Pak column (100 mg). Prior to MS analysis, the DNA was precipitated from ammonium acetate (pH 5.6) at -80 °C.

1. Yadav, J. S.; Nirranjan Kumar, N.; Sridhar Reddy, M.; Prasad, A. R. *Tetrahedron* **2007**, *63*, 2689-2694.
2. Abushanab, E.; Vemishetti, P.; Leiby, R. W.; Singh, H. K.; Mikkilineni, A. B.; Wu, D. C. J.; Saibaba, R.; Panzica, R. P. *J. Org. Chem.* **1988**, *53*, 2598-2602.
3. Mulzer, J.; Angermann, A.; Münch, W. *Liebigs Ann. Chem.* **1986**, 825-838.
4. Dhar, S.; Komada, T.; Greenberg, M. M. *J. Am. Chem. Soc.* **2007**, *129*, 8702-8703.
5. Mueller, R.; Yang, J.; Duan, C.; Pop, E.; Zhang, L. H.; Huang, T.-B.; Denisenko, A.; Denisko, O. V.; Oniciu, D. C.; Bisgaier, C. L.; Pape, M. E.; Freiman, C. D.; Goetz, B.; Cramer, C. T.; Hopson, K. L.; Dasseux, J.-L. *J. Med. Chem.* **2004**, *47*, 5183-5197.
6. Bae, S.; Lakshman, M. K. *J. Org. Chem.* **2008**, *73*, 3707-3713.

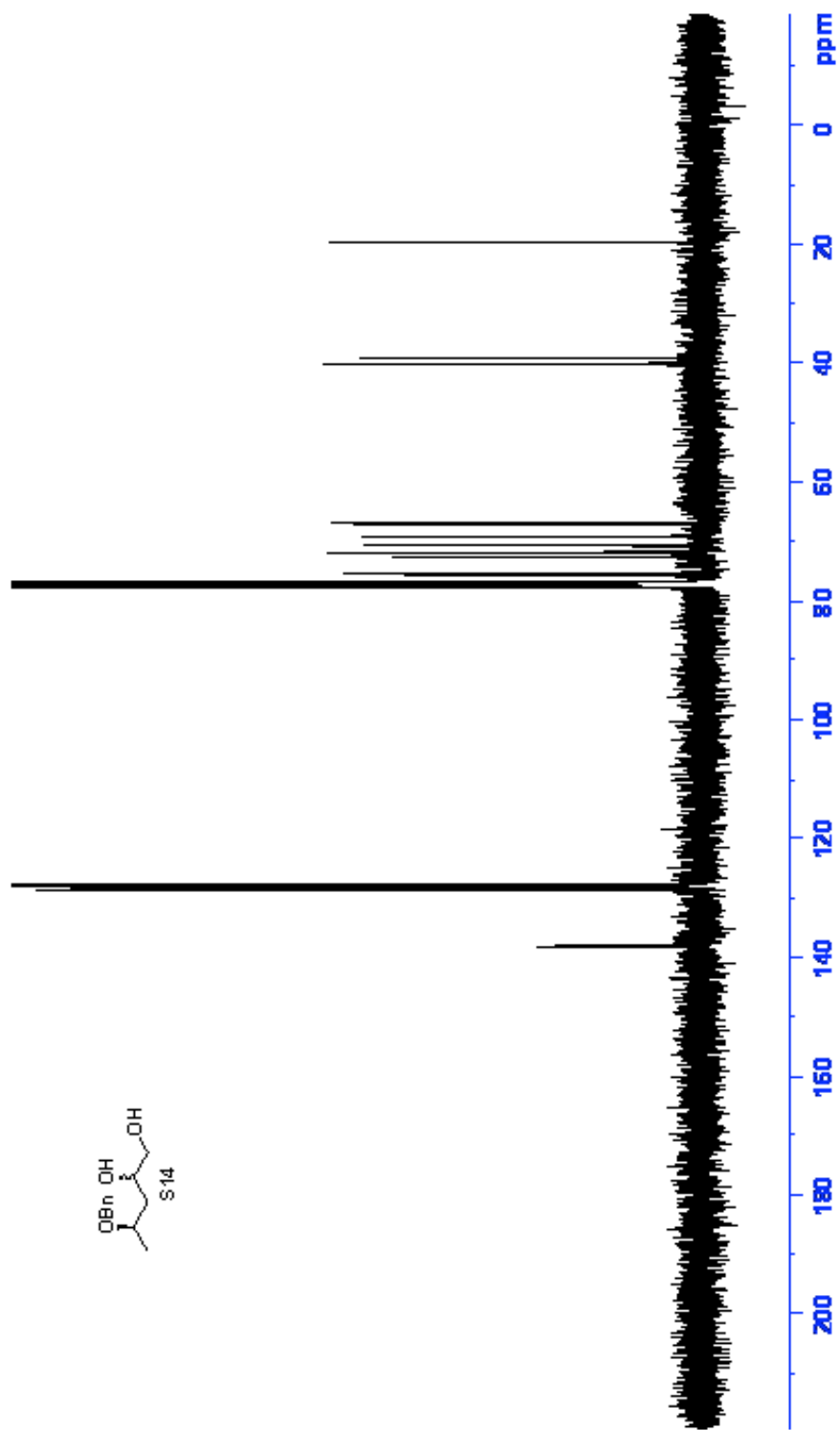


Supporting Information Figure 1. ¹H NMR spectrum of S13.

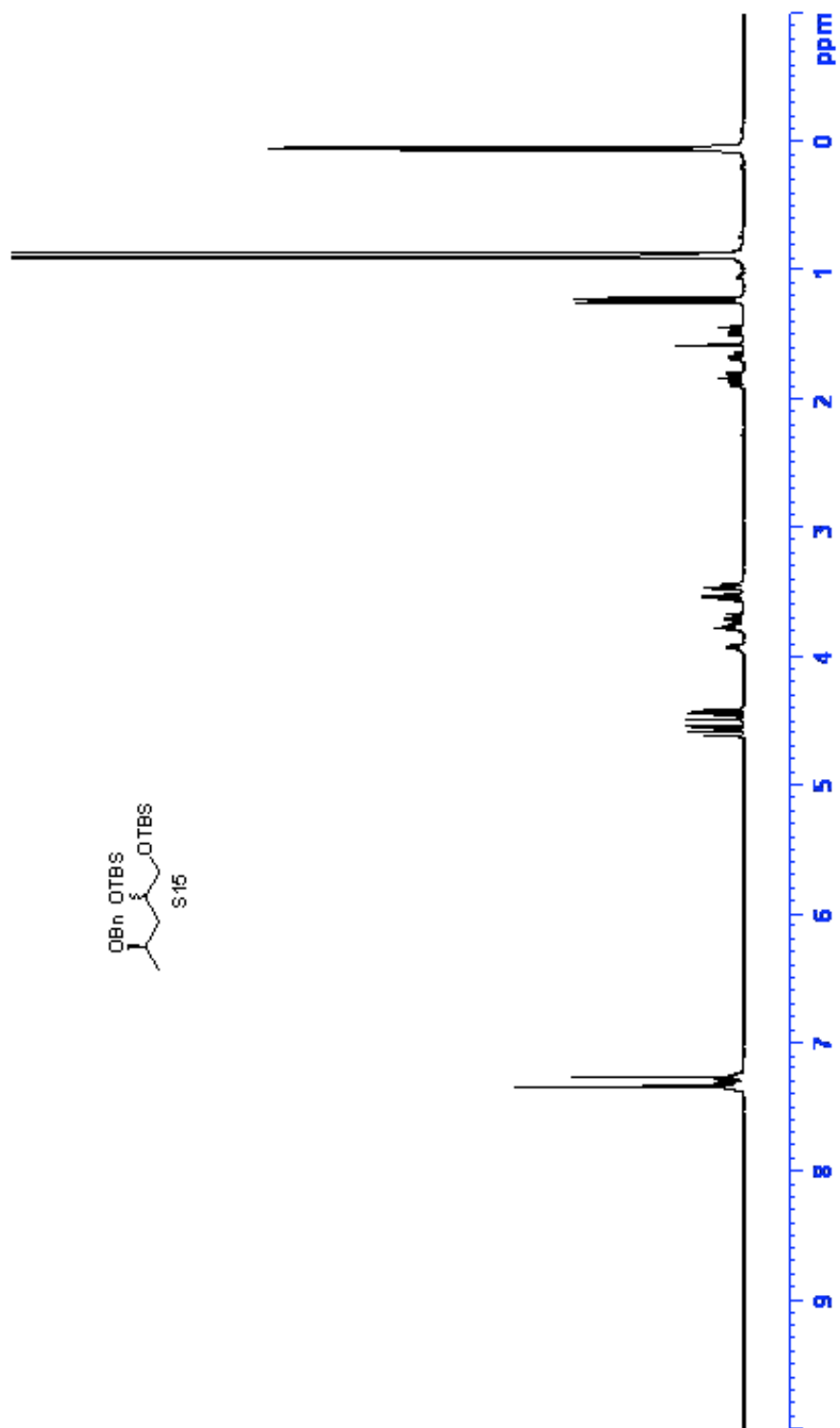




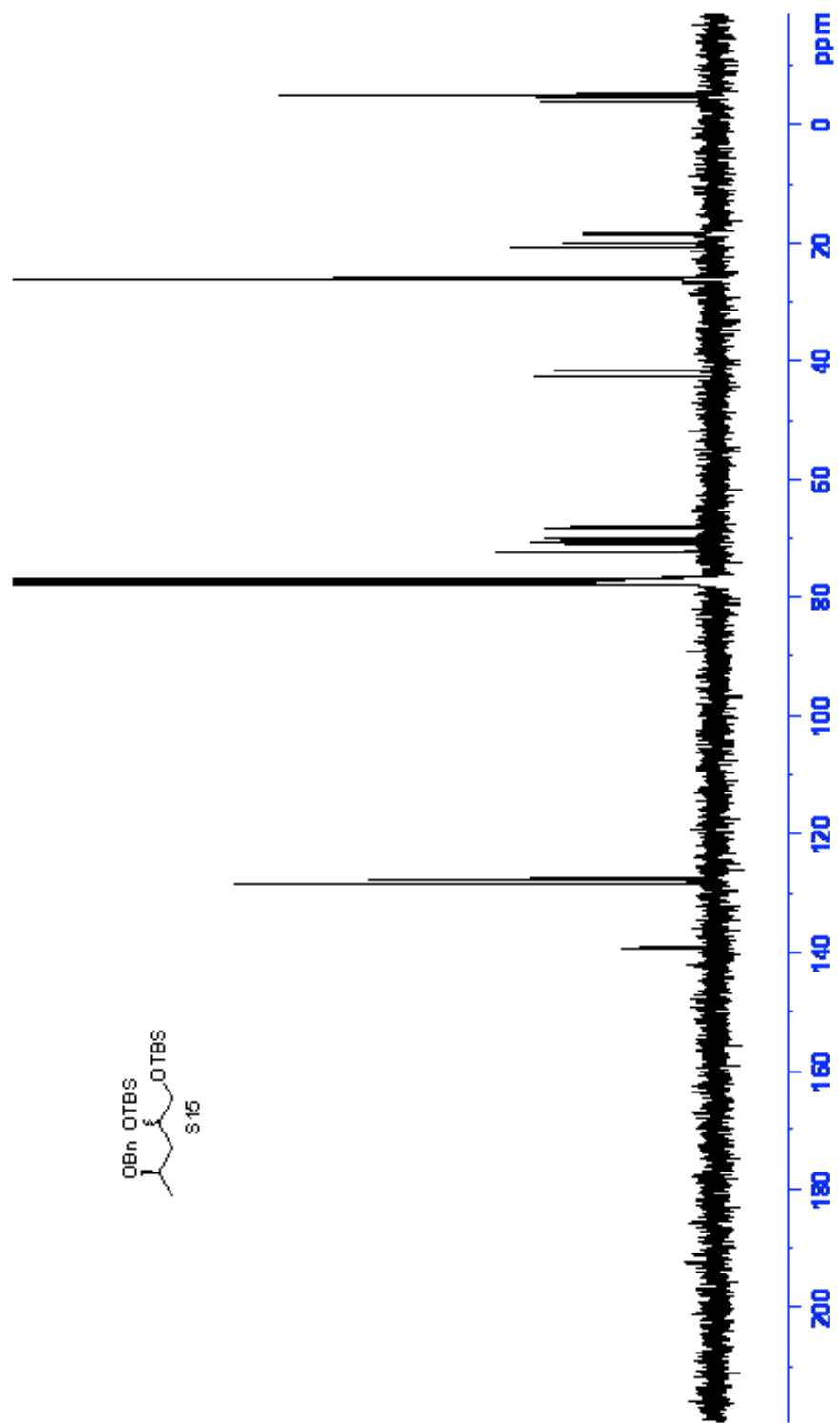
Supporting Information Figure 3. ^1H NMR spectrum of S14.



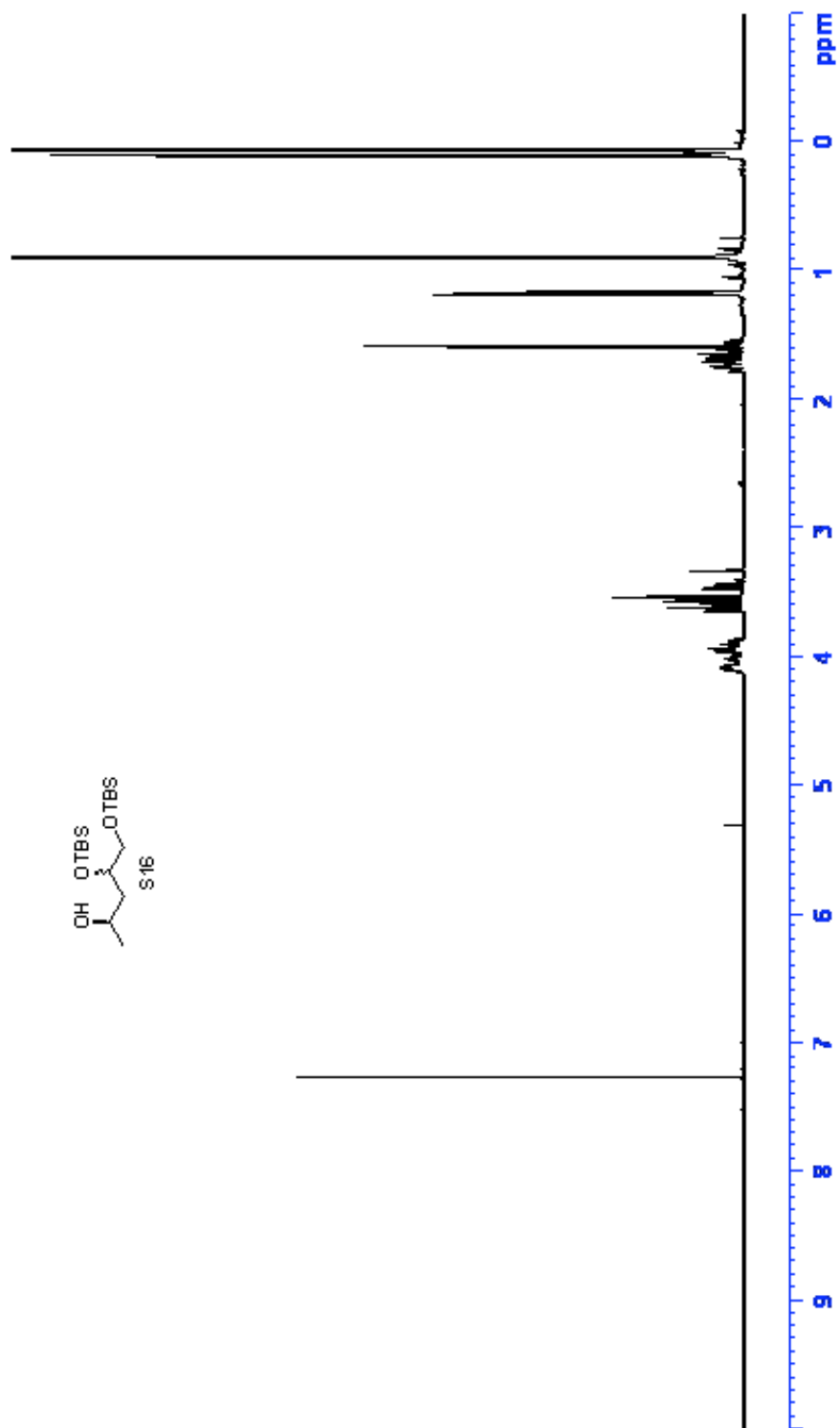
Supporting Information Figure 4. ^{13}C NMR spectrum of S14.



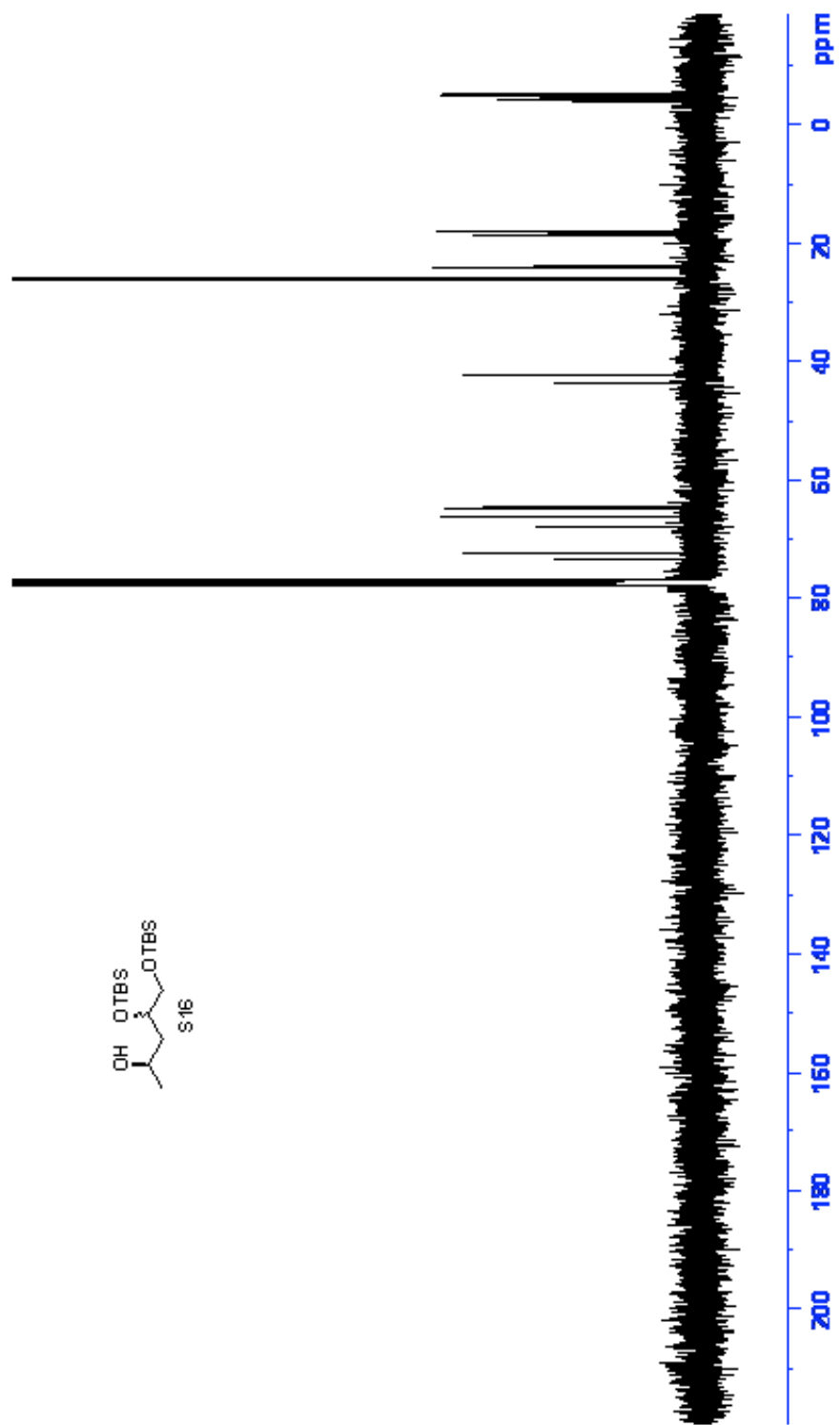
Supporting Information Figure 5. ^1H NMR spectrum of S15.



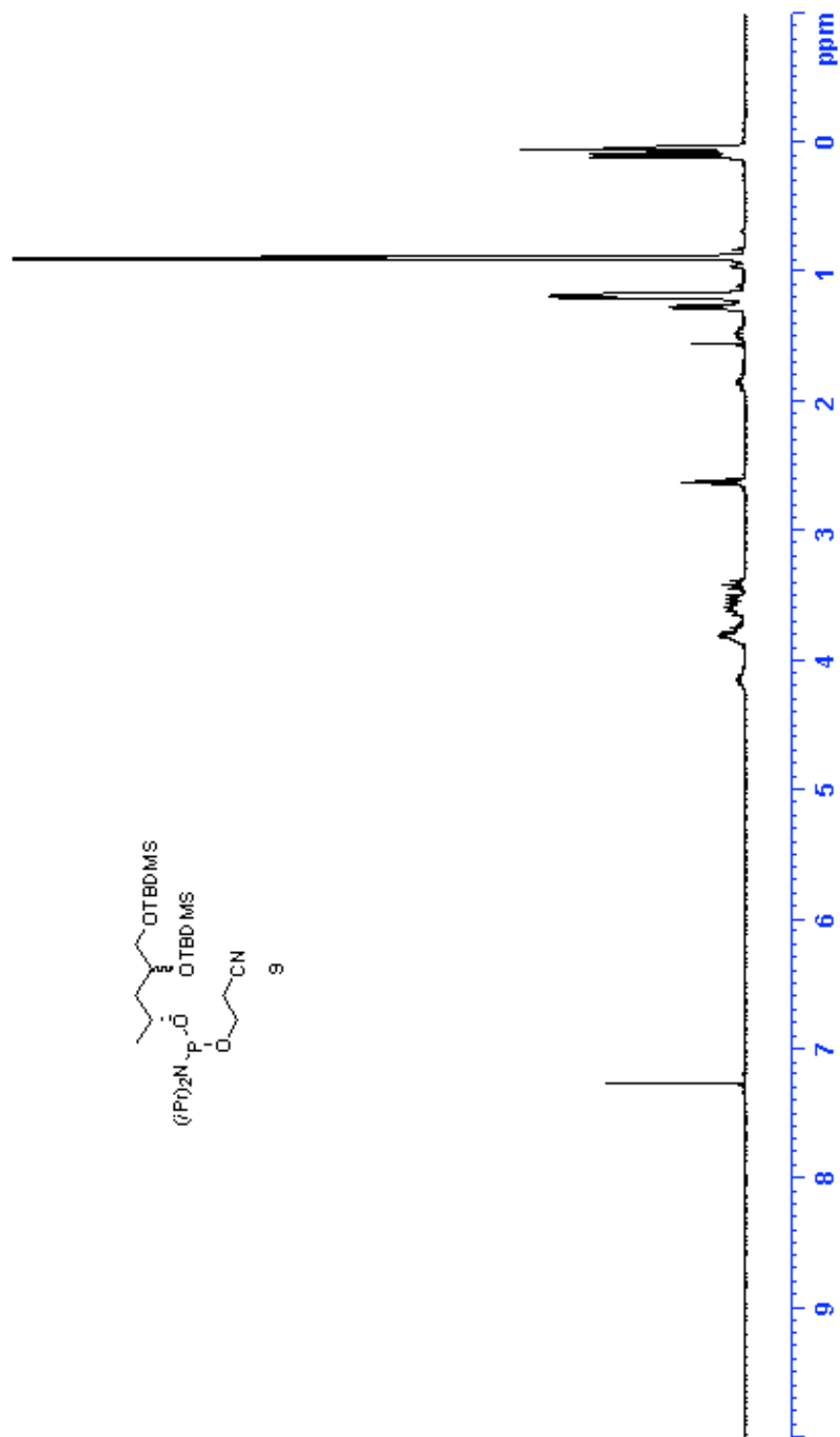
Supporting Information Figure 6. ^{13}C NMR spectrum of S15.



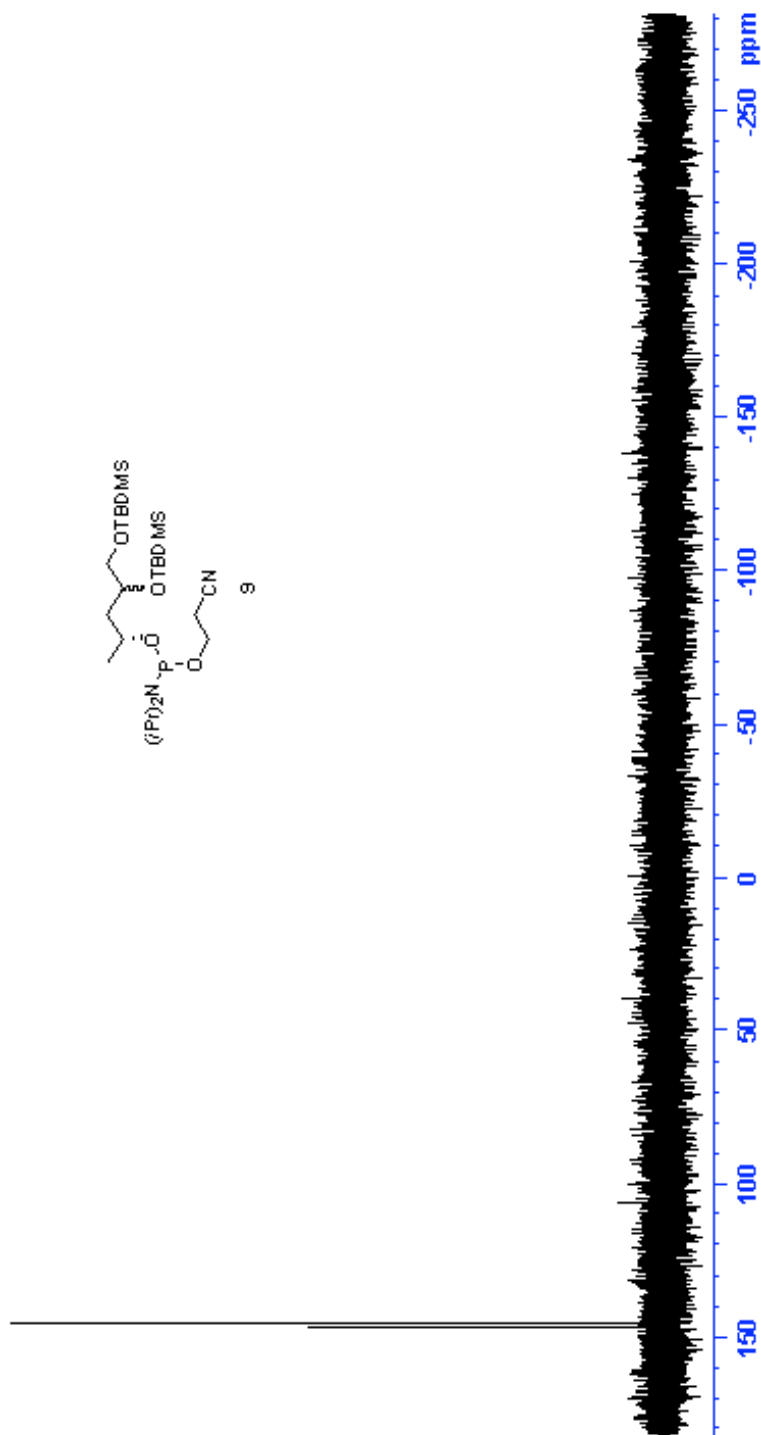
Supporting Information Figure 7. ^1H NMR spectrum of **S16**.



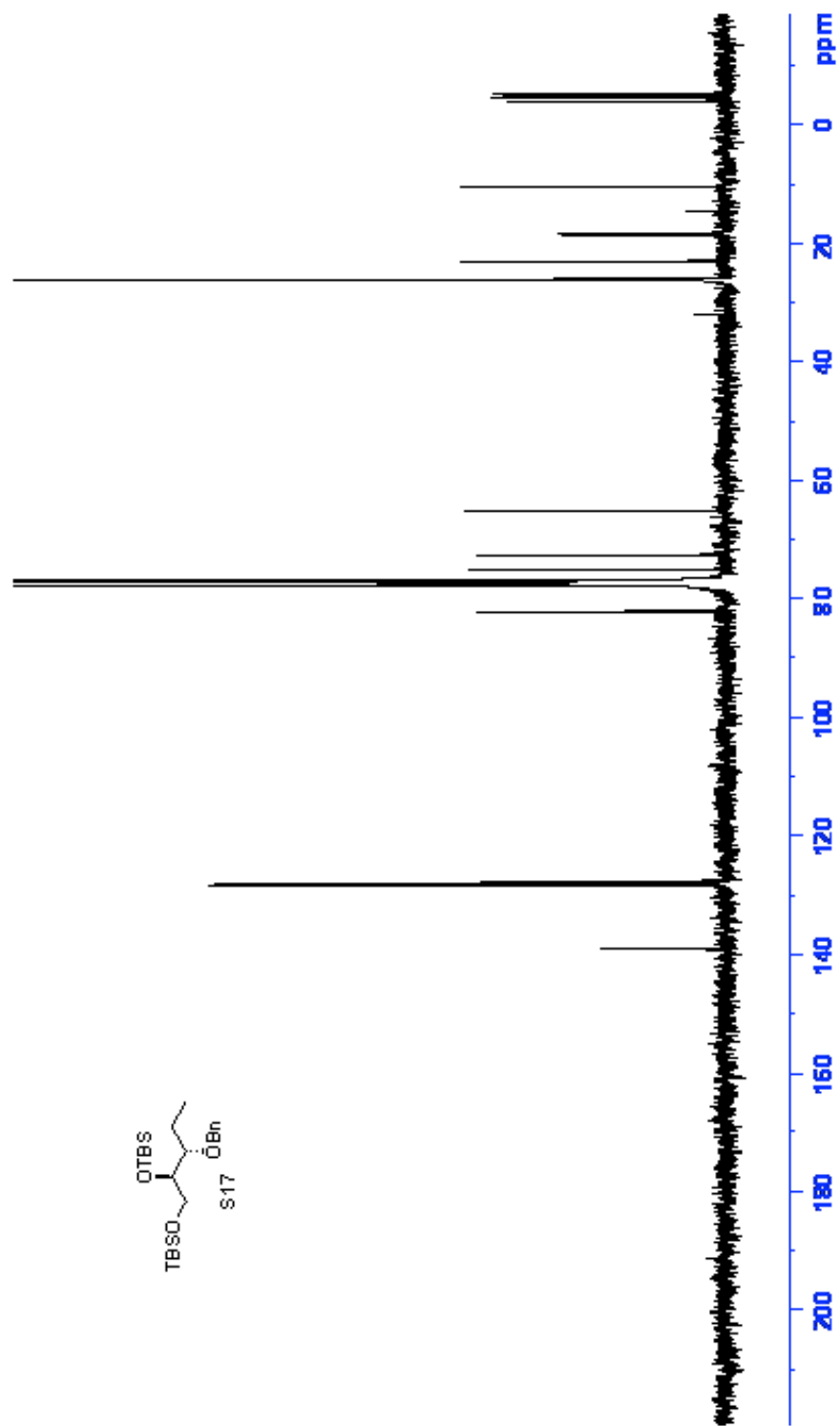
Supporting Information Figure 8. ¹³C NMR spectrum of S16.



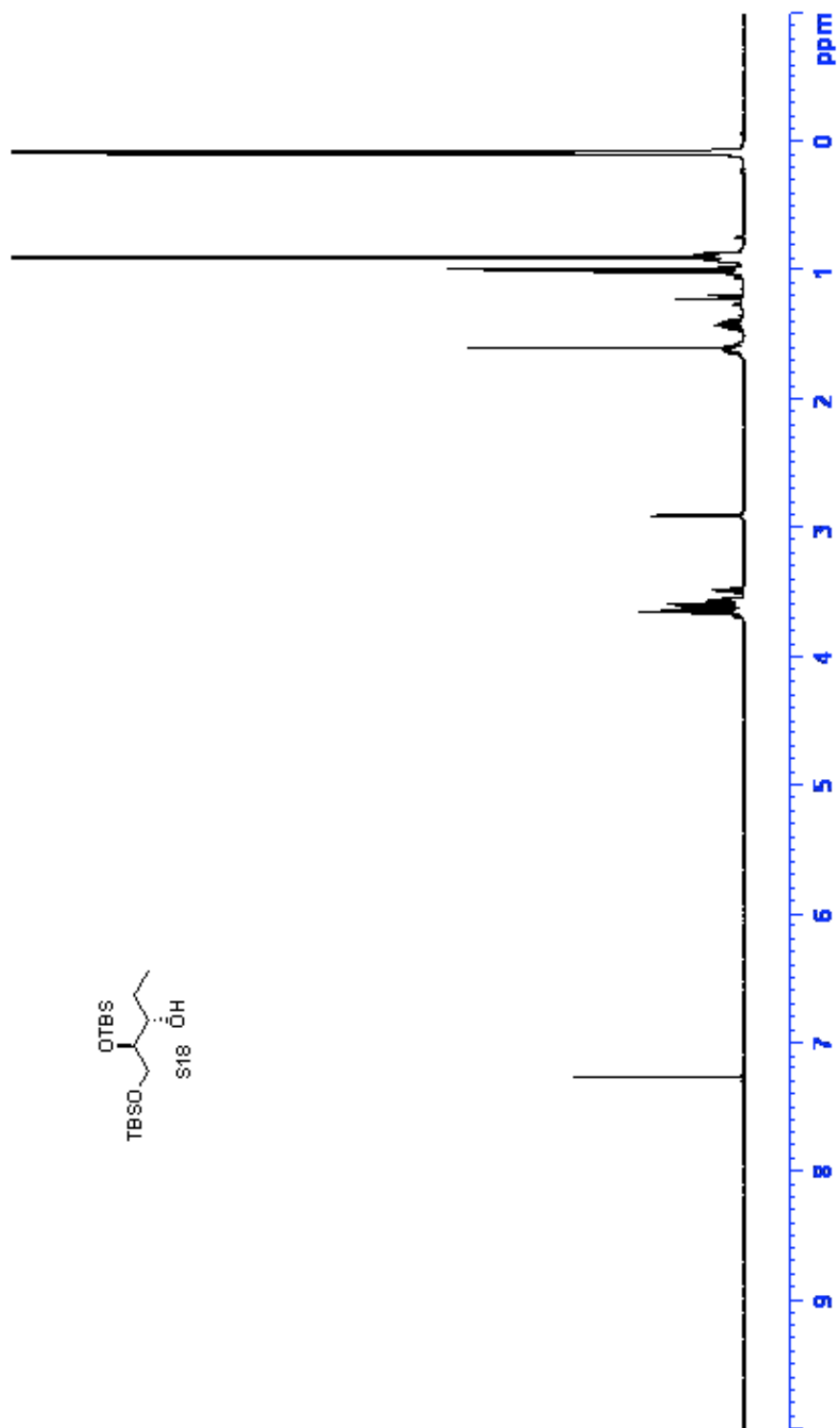
Supporting Information Figure 9. ^1H NMR spectrum of **9**.



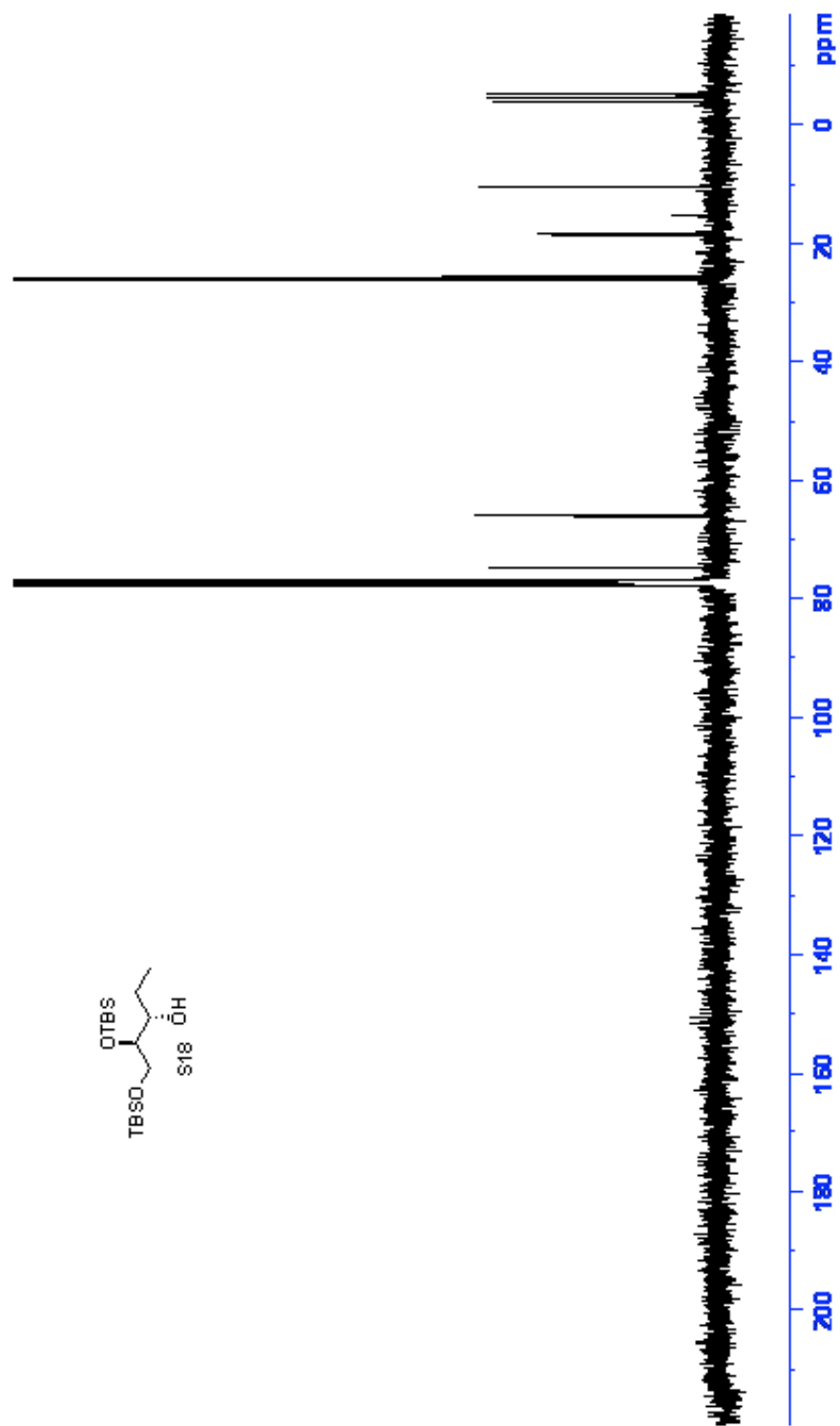
Supporting Information Figure 10. ^{31}P NMR spectrum of **9**.



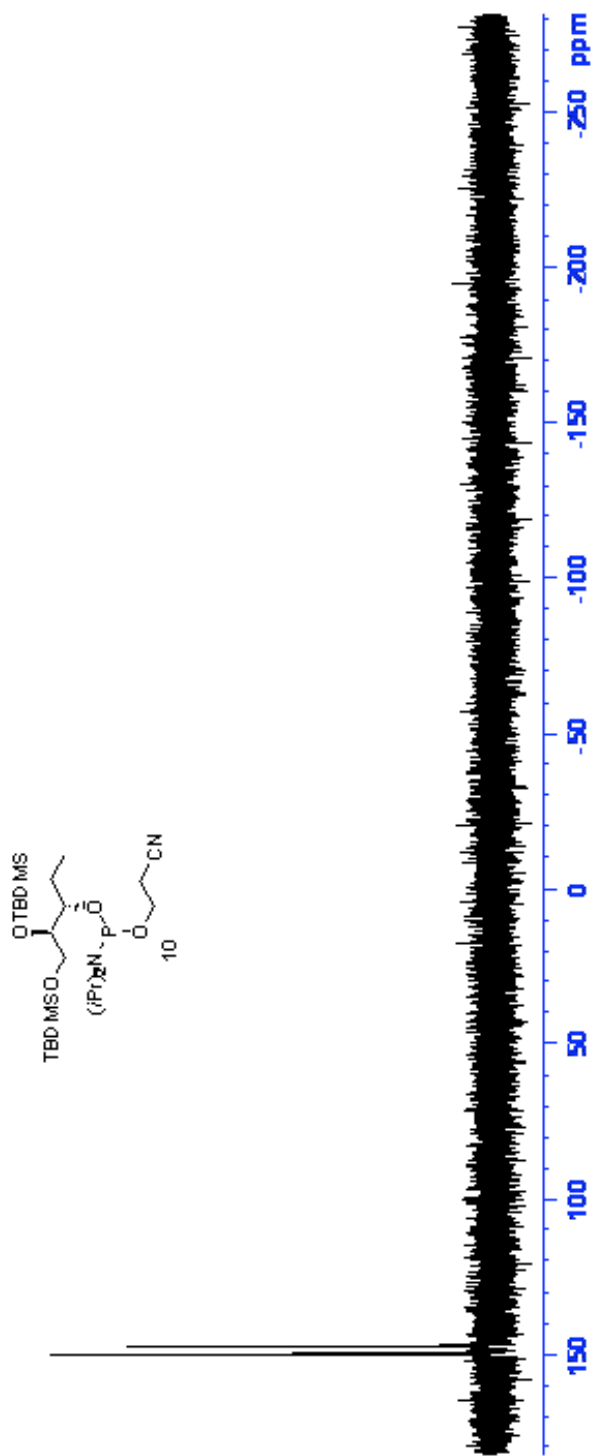
Supporting Information Figure 12. ¹³C NMR spectrum of S17.



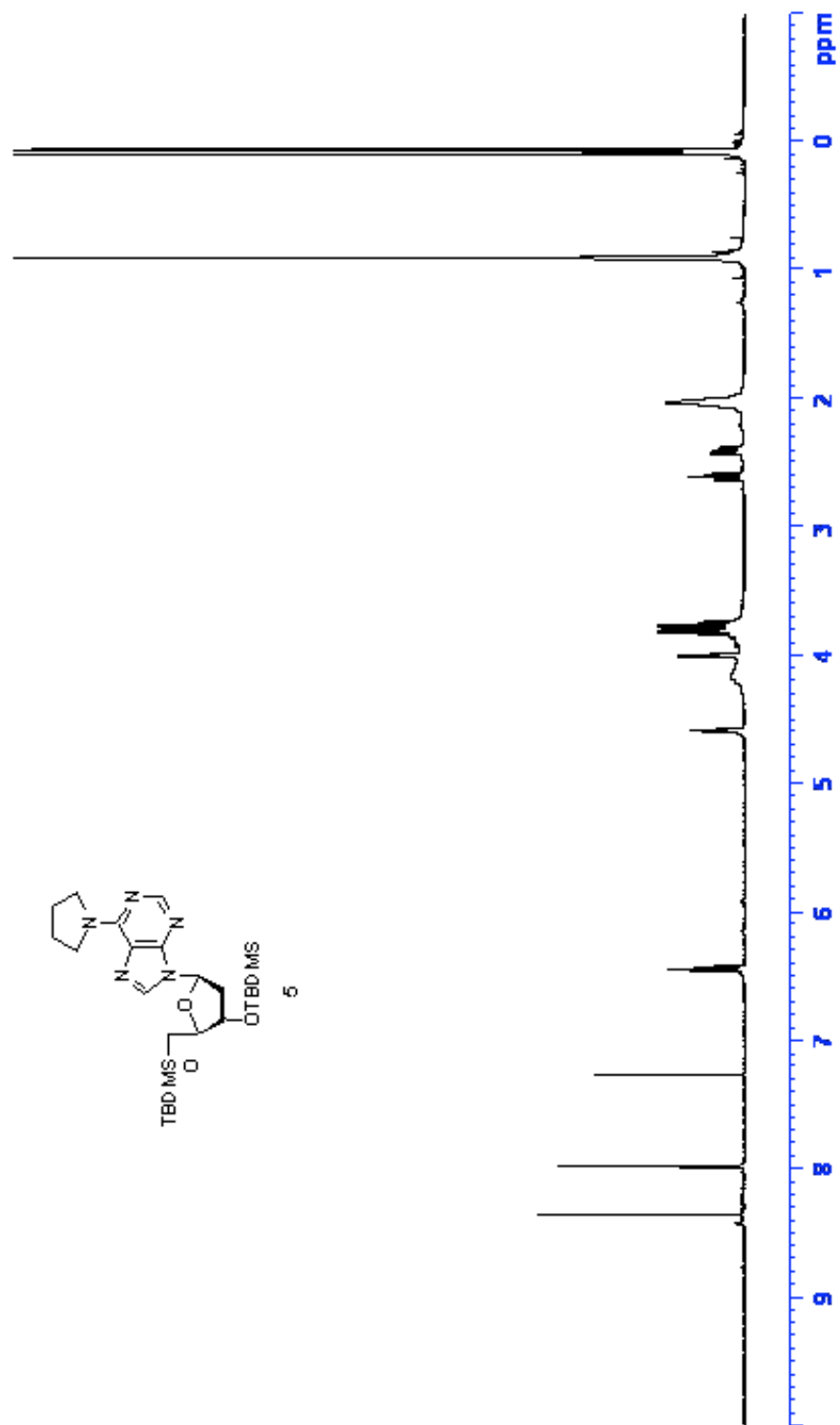
Supporting Information Figure 13. ¹H NMR spectrum of S18.



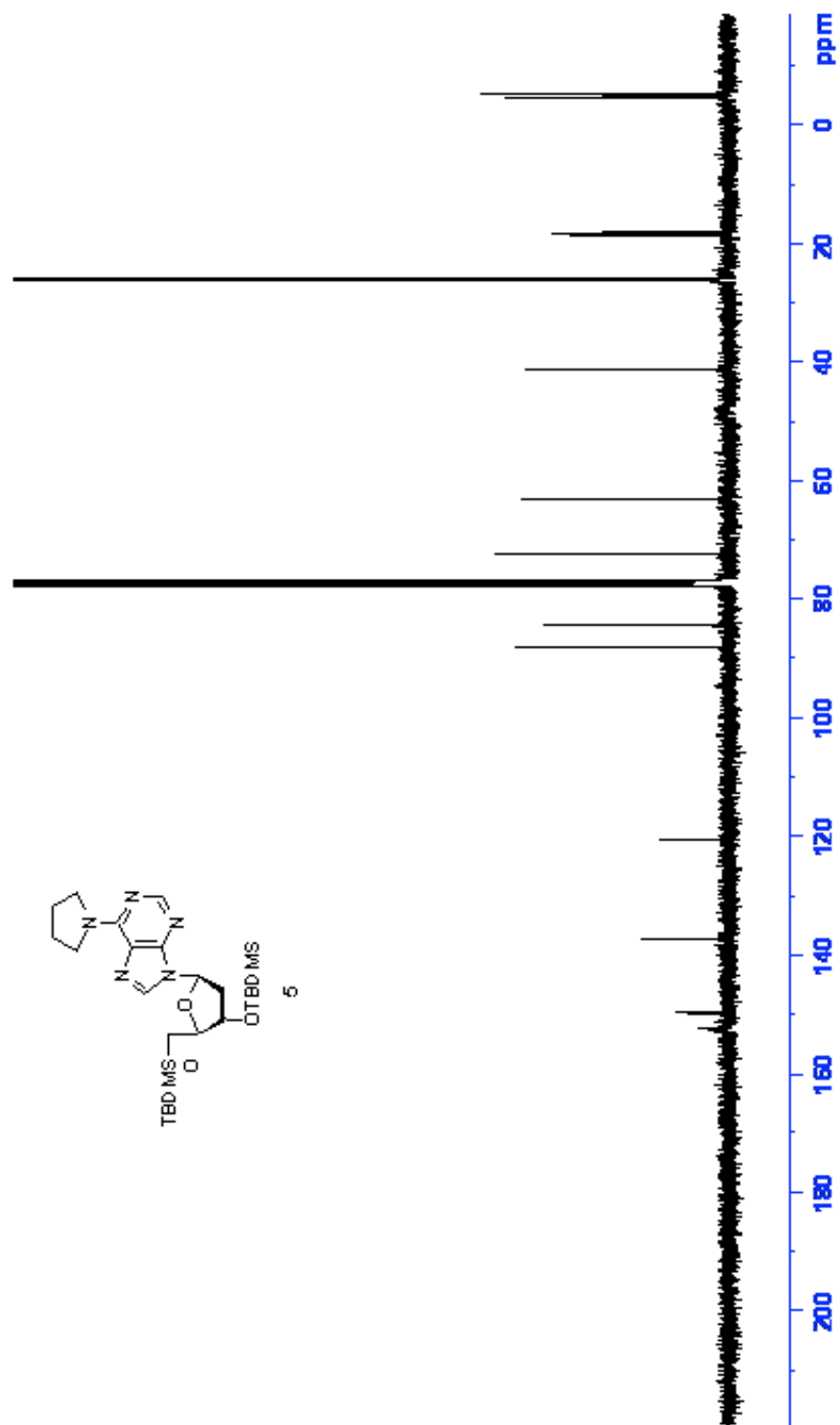
Supporting Information Figure 14. ¹³C NMR spectrum of S18.



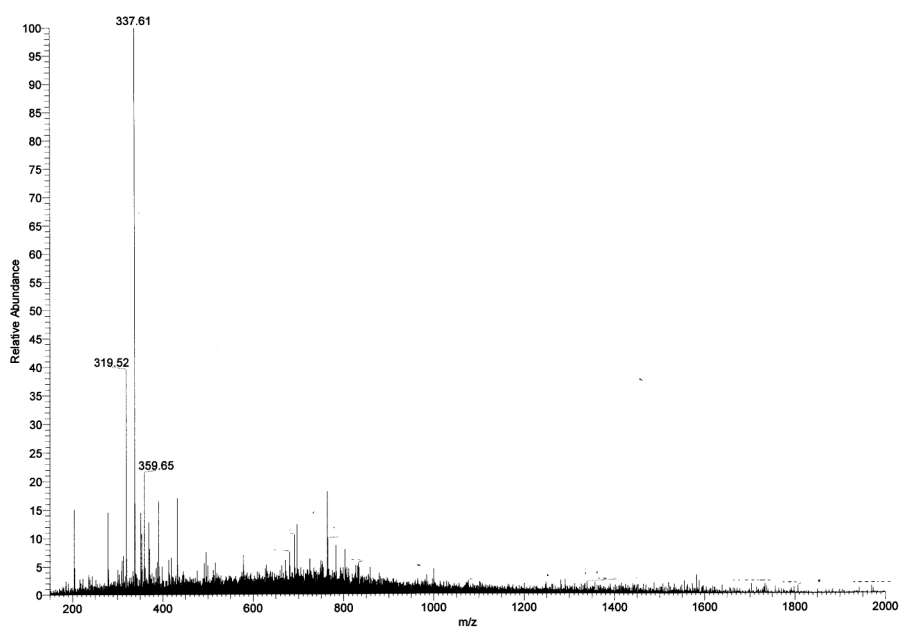
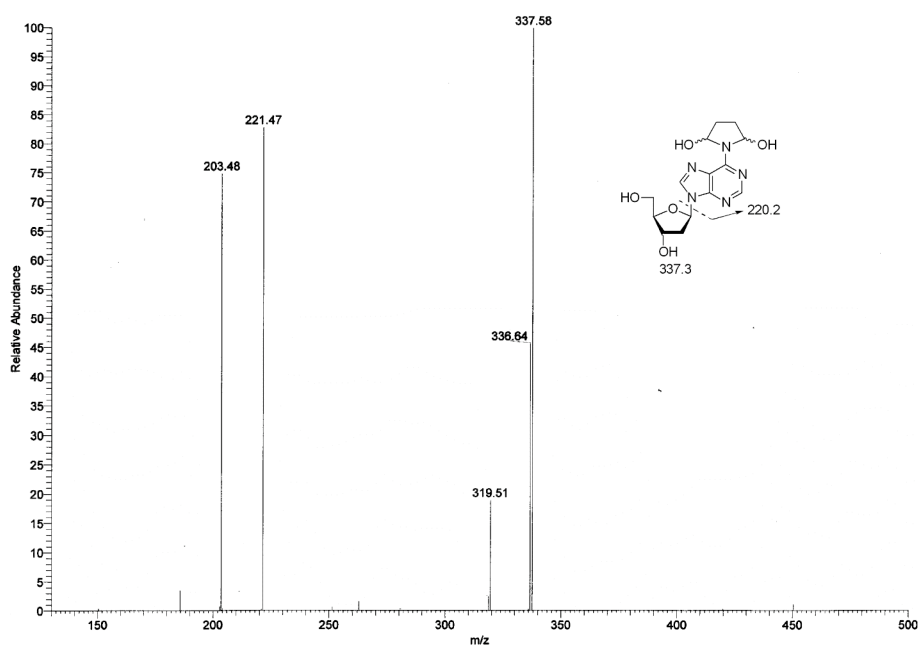
Supporting Information Figure 16. ^{31}P NMR spectrum of 10.



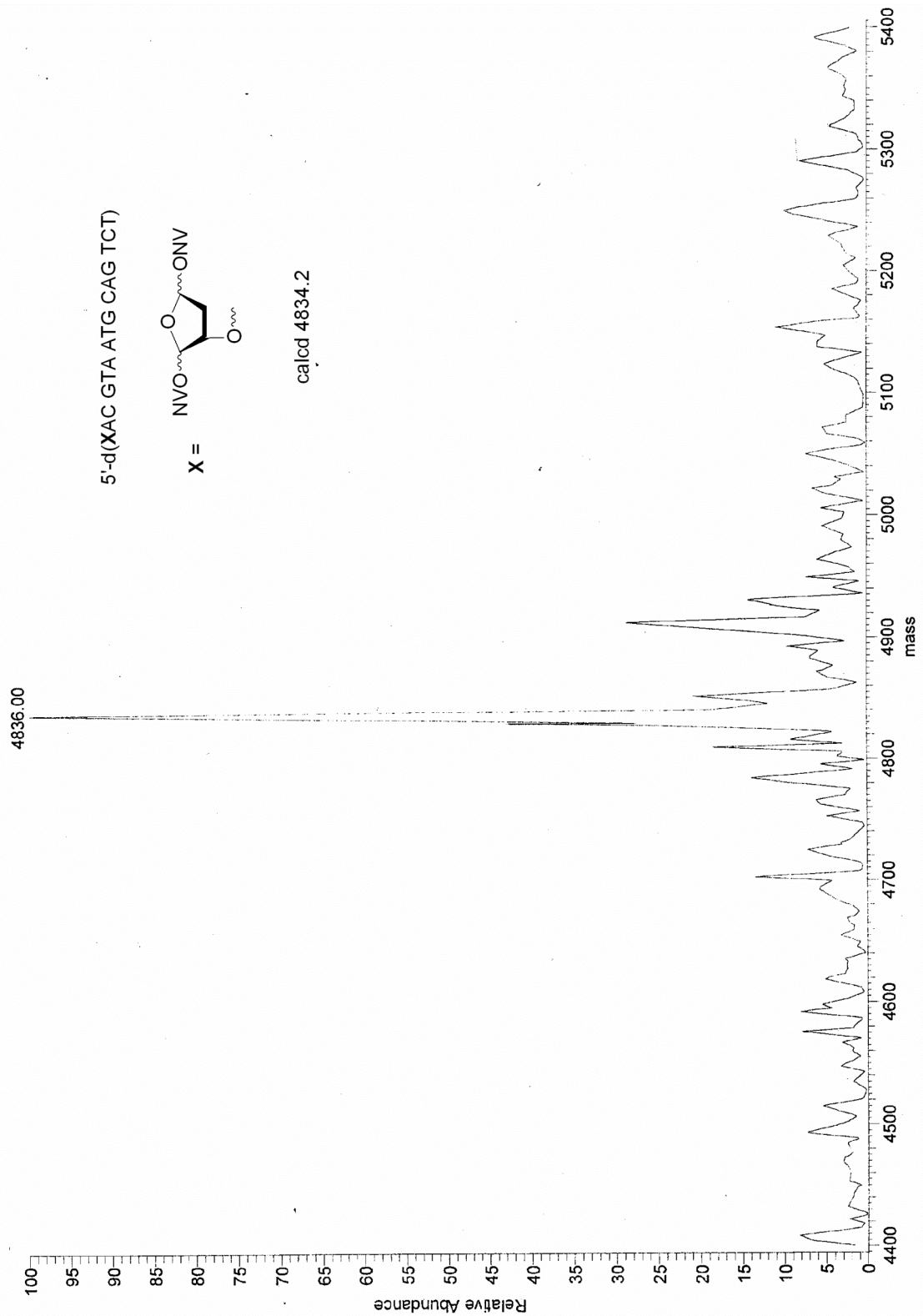
Supporting Information Figure 17. ¹H NMR spectrum of **5**.



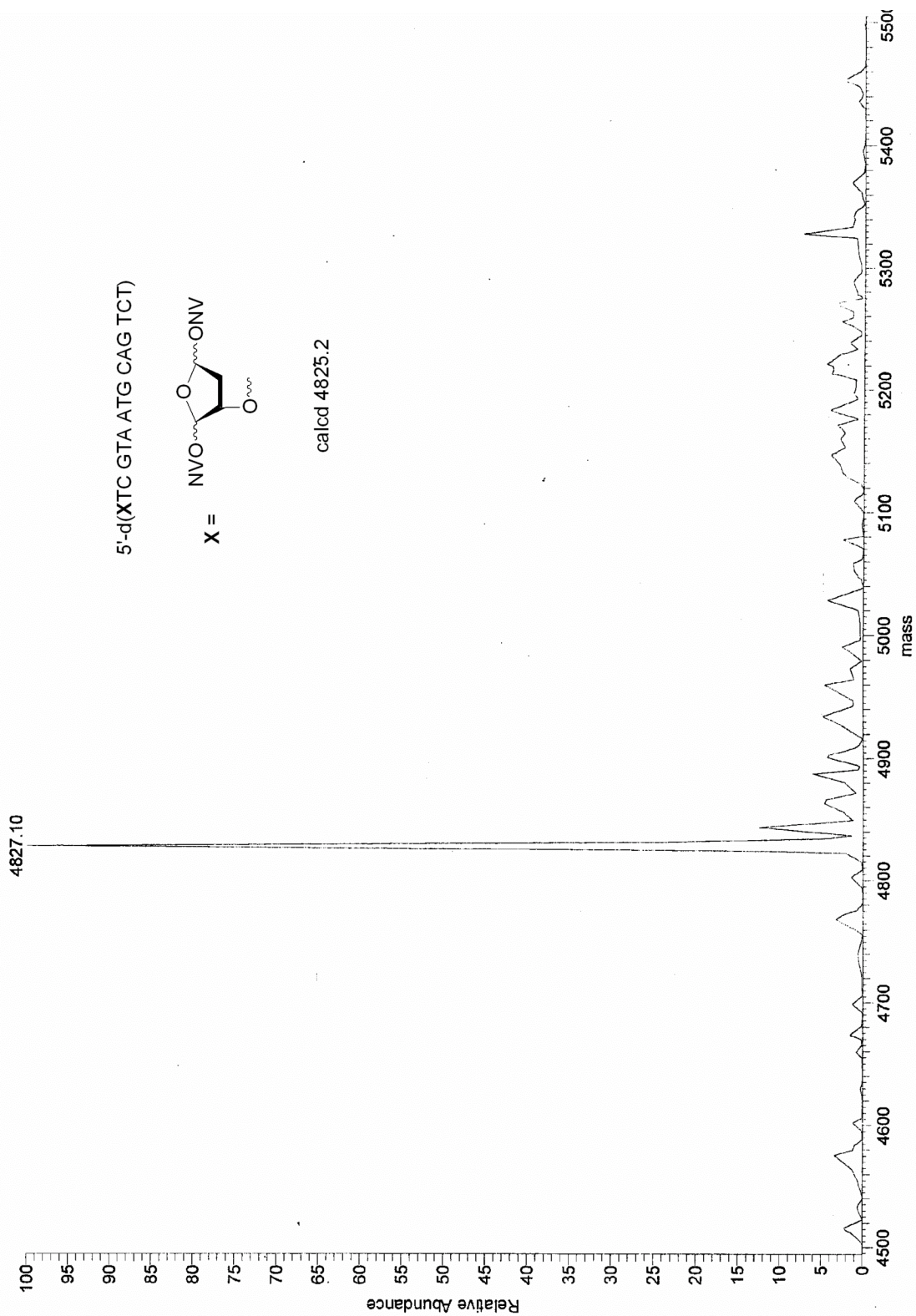
Supporting Information Figure 18. ^1H NMR spectrum of **5**.

A**B**

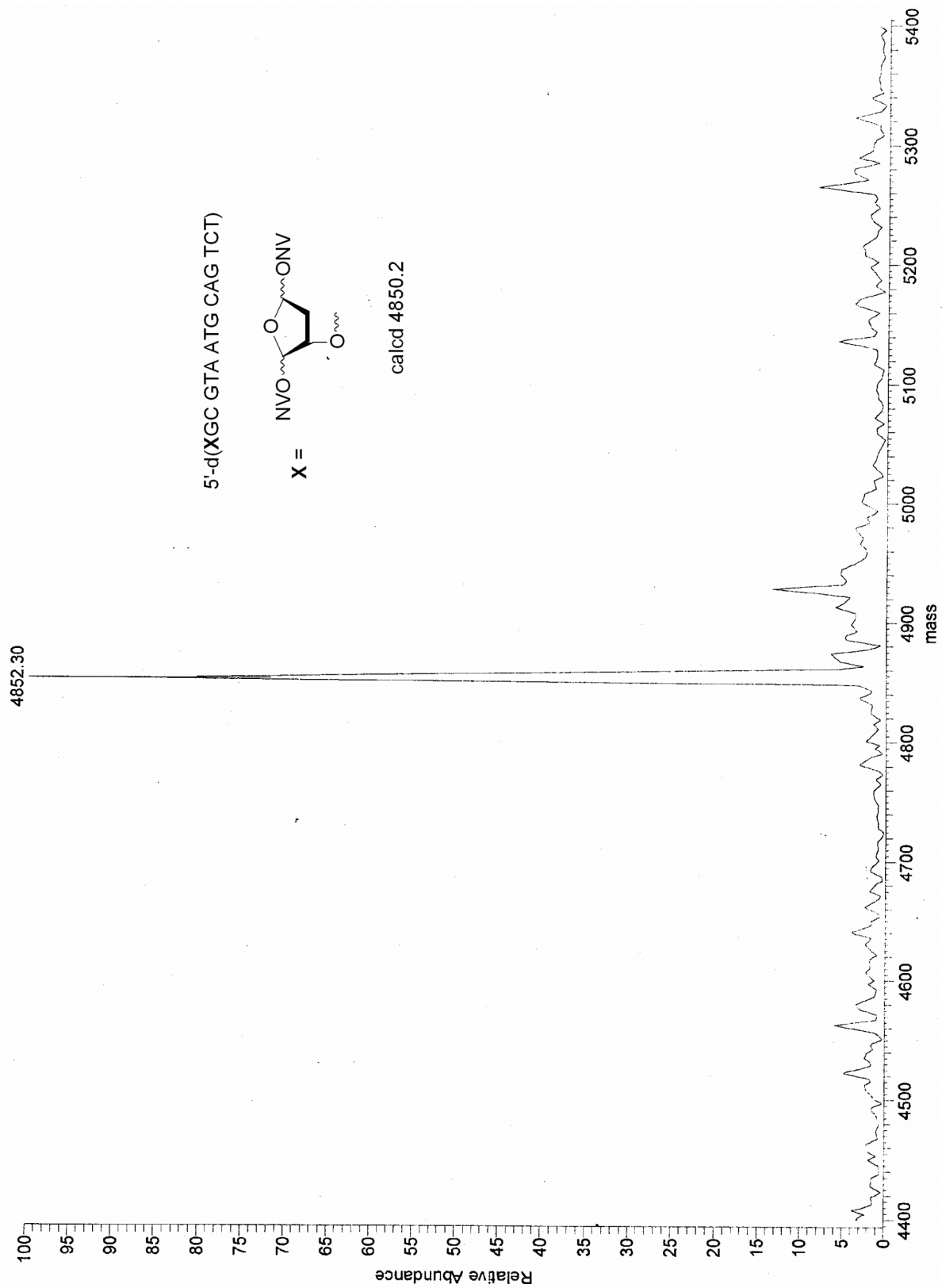
Supporting Information Figure 19. ESI-MS/MS of **4**. A) Full-view ESI spectrum of **4**. B) MS/MS fragmentation performed on the peak at 337.6 *m/z*. Peak at 319.5 *m/z* is $[M - H_2O]^+$. Peak at 203.5 *m/z* is the ion formed when $[M - H_2O]^+$ loses the 2'-deoxyribose moiety.



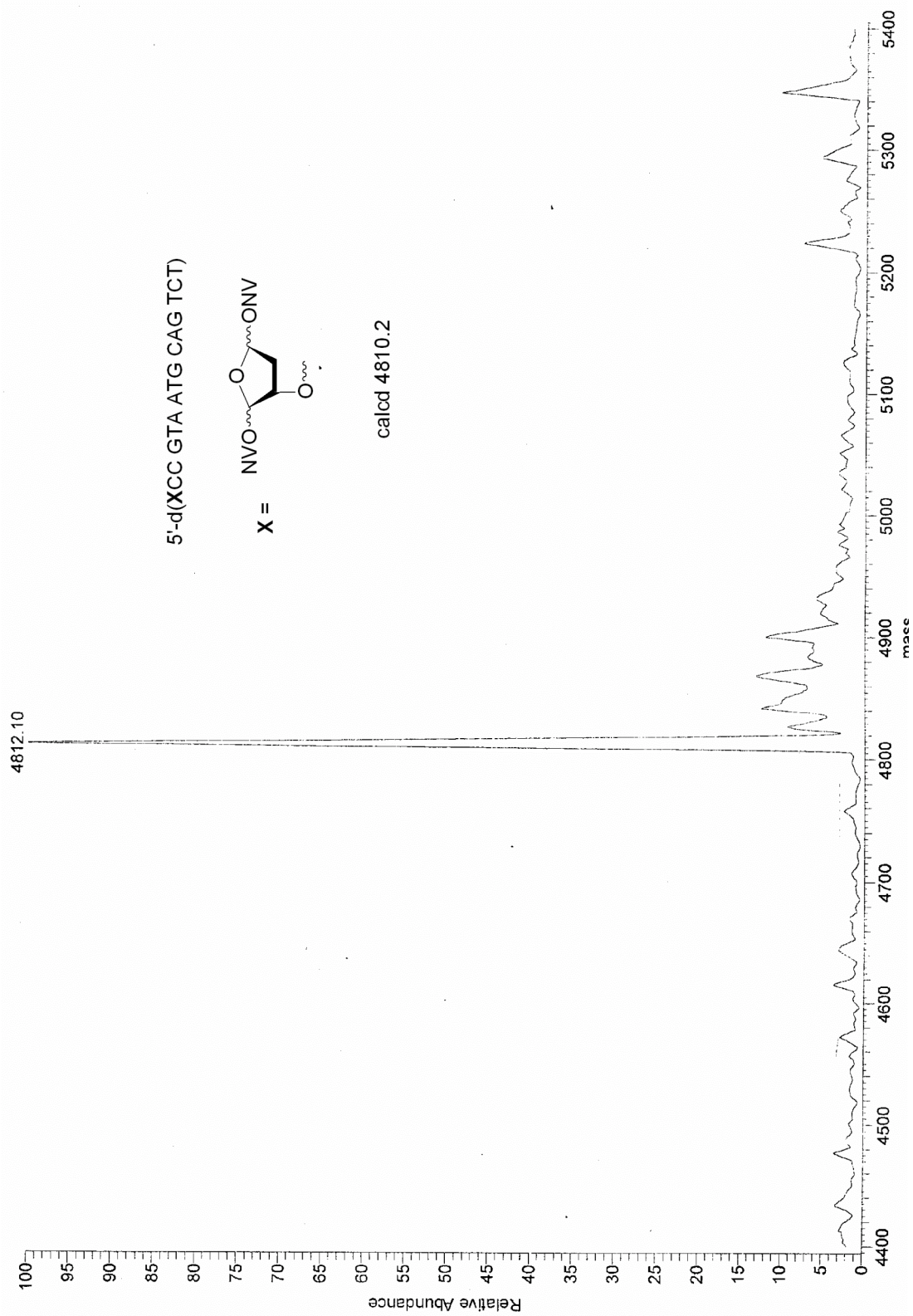
Supporting Information Figure 20. ESI-MS of oligonucleotide containing the DOB precursor (local sequence: 5'-XAC).



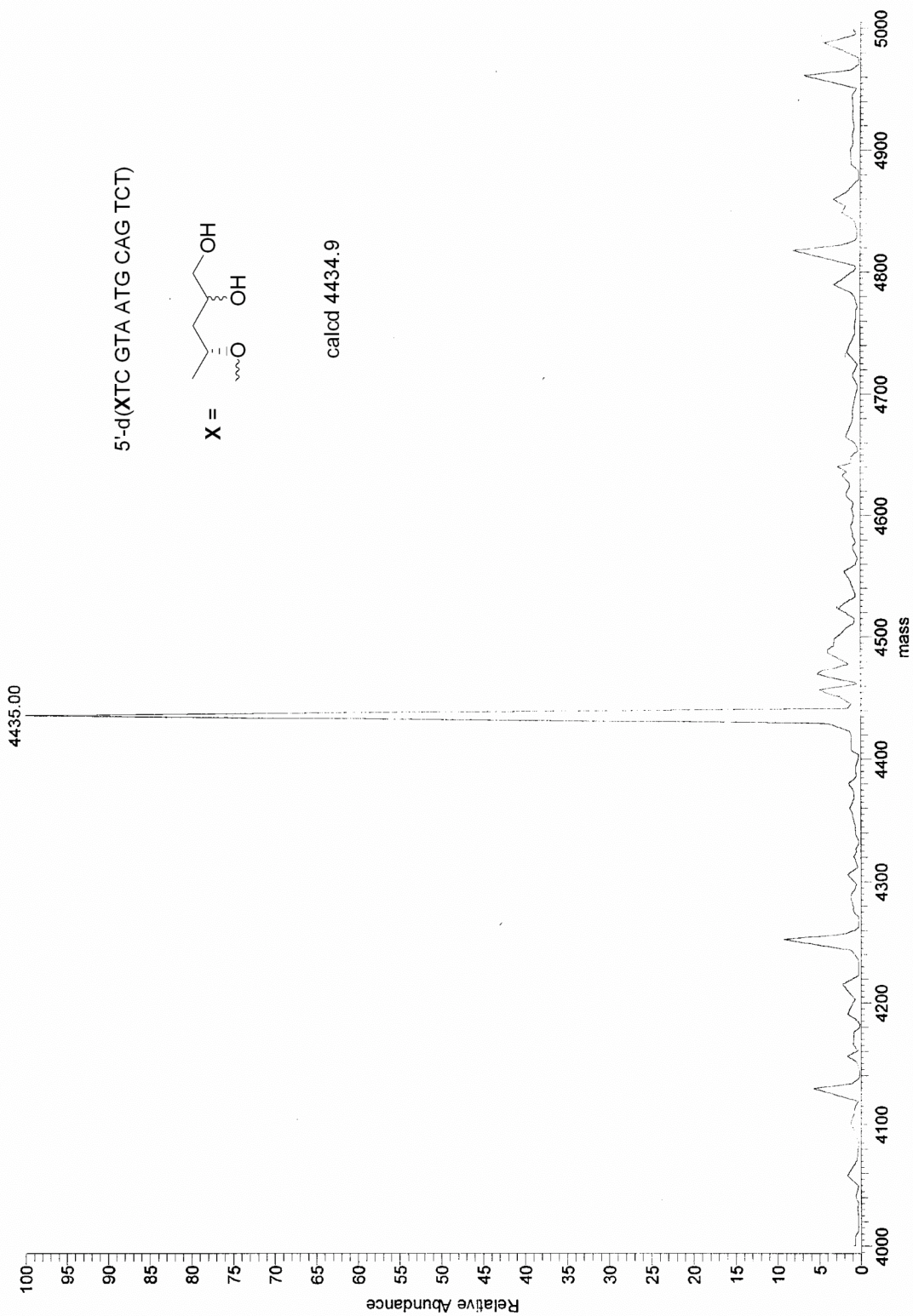
Supporting Information Figure 21. ESI-MS of oligonucleotide containing the DOB precursor (local sequence: 5'-XTC).



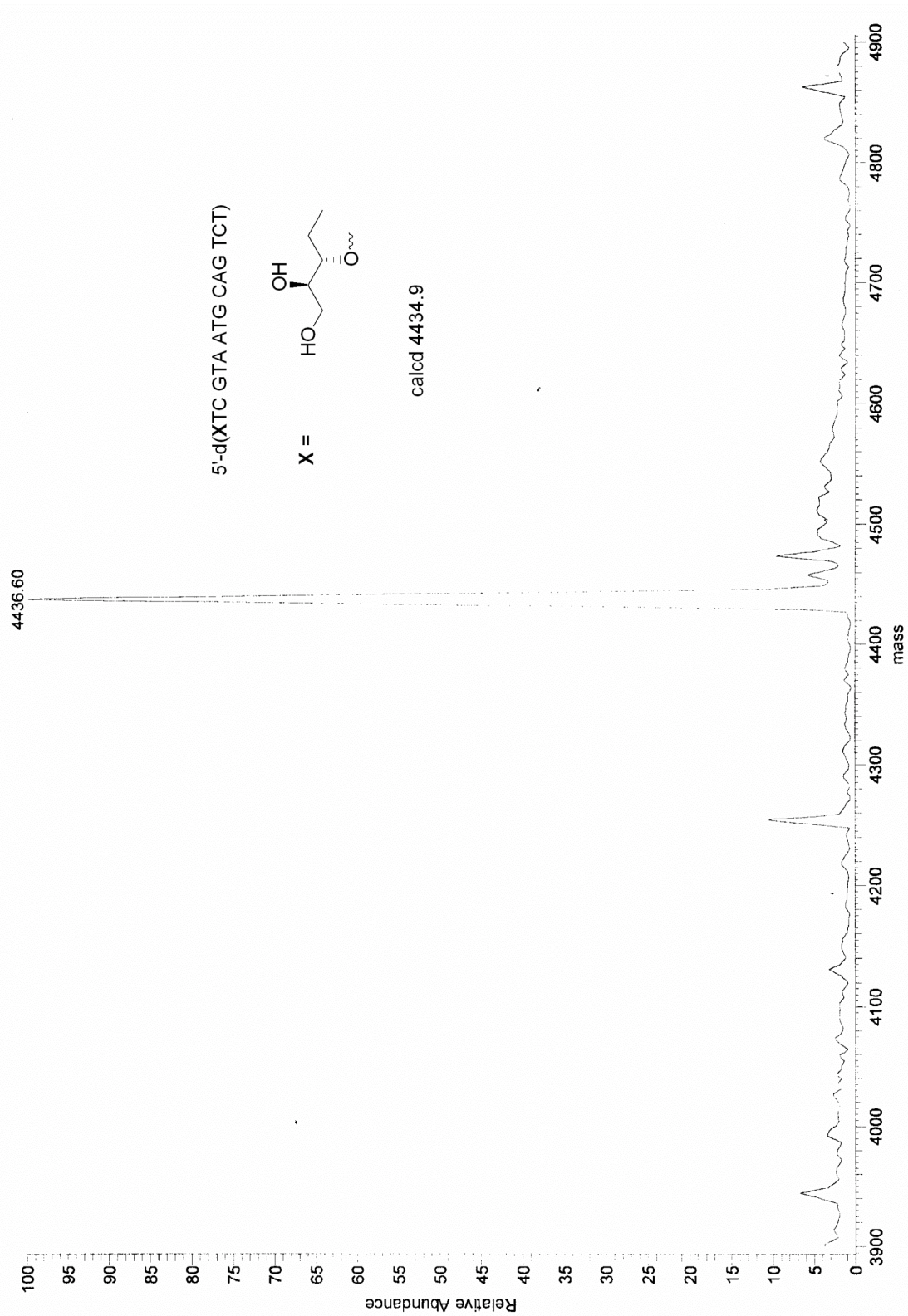
Supporting Information Figure 22. ESI-MS of oligonucleotide containing the DOB precursor (local sequence: 5'-XGC).



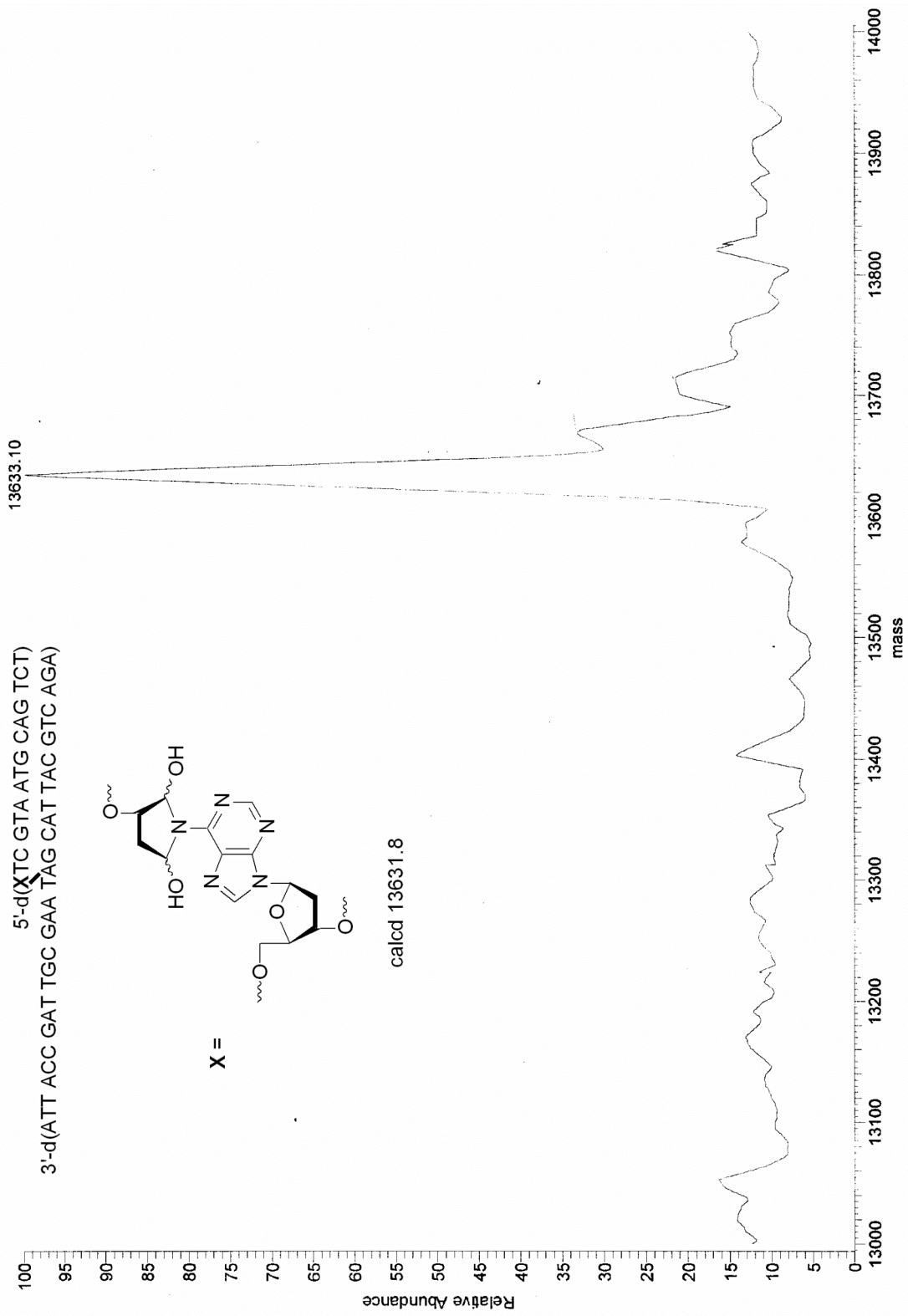
Supporting Information Figure 23. ESI-MS of oligonucleotide containing the DOB precursor (local sequence: 5'-XCC).



Supporting Information Figure 24. ESI-MS of oligonucleotide containing the precursor of **7** (local sequence: 5'-XTC).



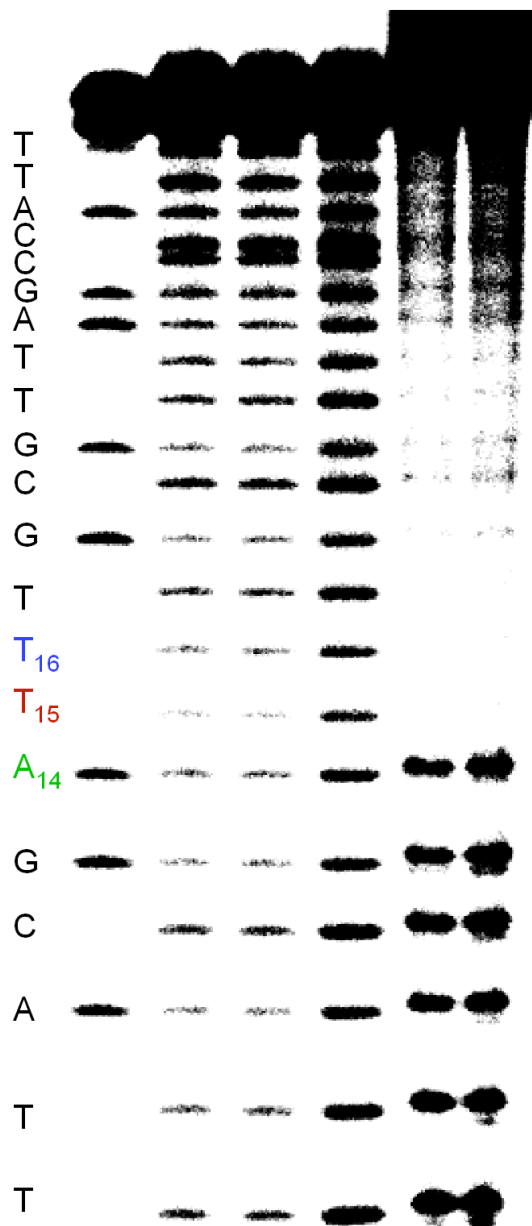
Supporting Information Figure 25. ESI-MS of oligonucleotide containing the precursor of **8** (local sequence: 5'-XTC).



Supporting Information Figure 26. ESI-MS of the ICL (**3k**) obtained from the ternary complex **2k**.

3a
 5'-d(DOB T₄₇C GTA ATG CAG TCT)
 3'-d(ATT ACC GAT TGC GTT₁₆ T₁₅ A₁₄G CAT TAC GTC AGA)

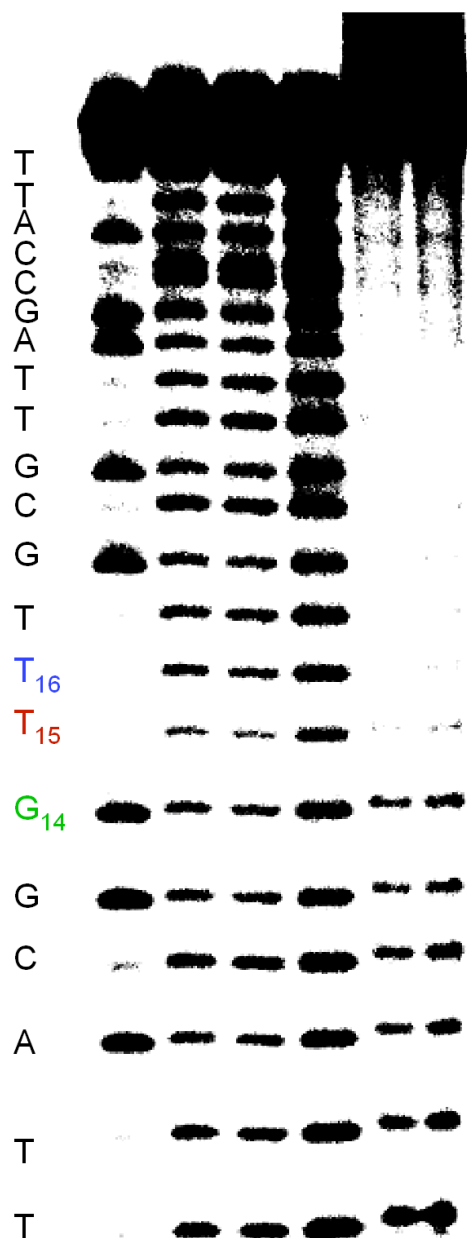
Time (min): 0.5 1 1 2 3
 Lane: 1 2 3 4 5 6



Supporting Information Figure 27. Hydroxyl radical cleavage of **3a**. **2a** (lanes 2-4) and **3a** (5-6) were treated with OH• for the indicated time. Lane 1; G/A sequencing of **2a**.

3c
 5'-d(DOB C₄₇C GTA ATG CAG TCT)
 3'-d(ATT ACC GAT TGC GTT₁₆ T₁₅ G₁₄G CAT TAC GTC AGA)

Time (min): 0.5 1 1 2 3
 Lane: 1 2 3 4 5 6

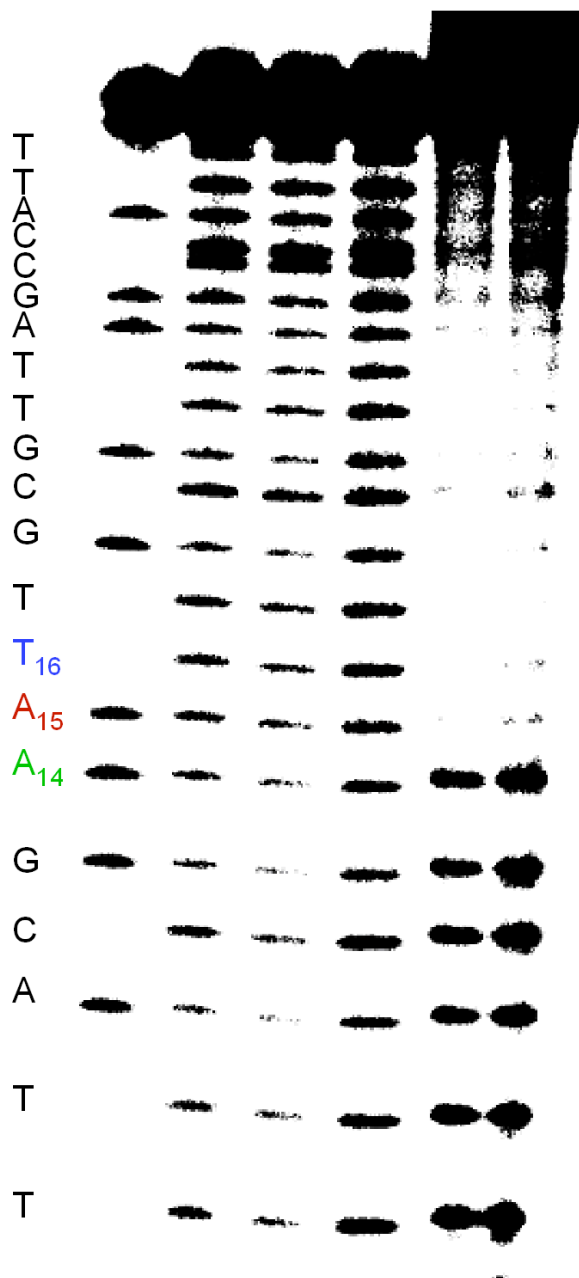


Supporting Information Figure 28. Hydroxyl radical cleavage of 3c. 2c (lanes 2-4) and 3c (lanes 5-6) were treated with OH• for the indicated time. Lane 1; G/A sequencing of 2c.

3i

5'-d(DOB T₄₇C GTA ATG CAG TCT)
3'-d(ATT ACC GAT TGC GTT₁₆ A₁₅ A₁₄G CAT TAC GTC AGA)

Time (min): 0.5 1 1 2 3
Lane: 1 2 3 4 5 6

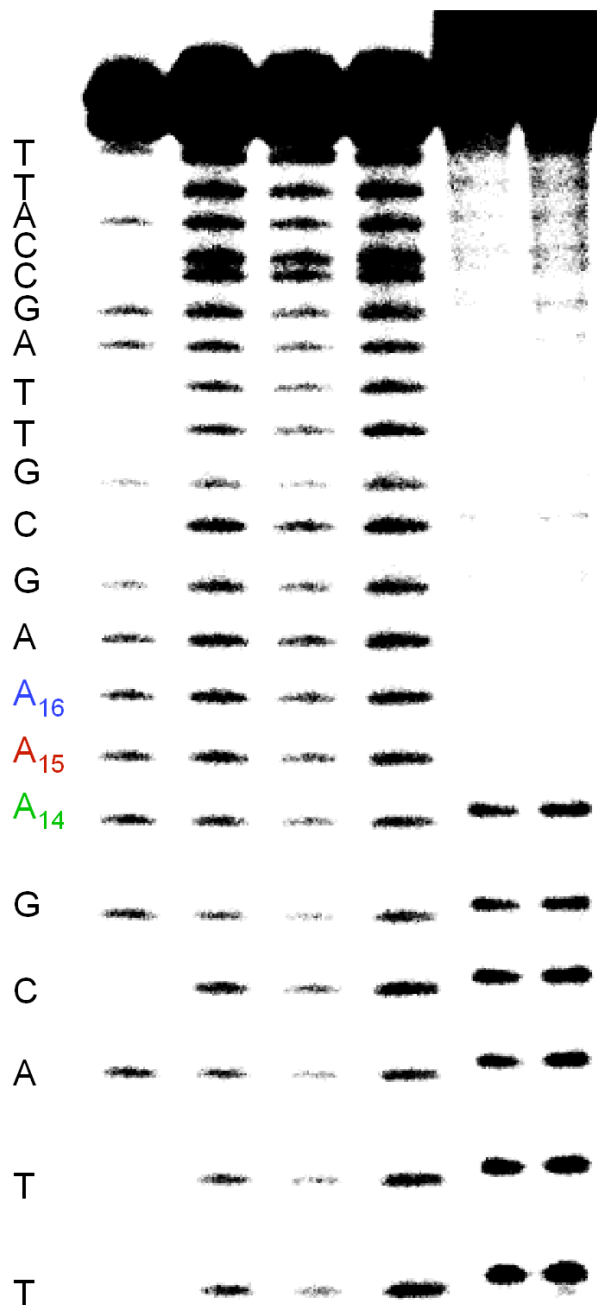


Supporting Information Figure 29. Hydroxyl radical cleavage of **3i**. **2i** (lanes 2-4) and **3i** (lanes 5-6) were treated with OH• for the indicated time. Lane 1; G/A sequencing of **2i**.

3j

5'-d(DOB T₄₇ C GTA ATG CAG TCT)
 3'-d(ATT ACC GAT TGC GAA_{A₁₆} A₁₅ A₁₄ G CAT TAC GTC AGA)

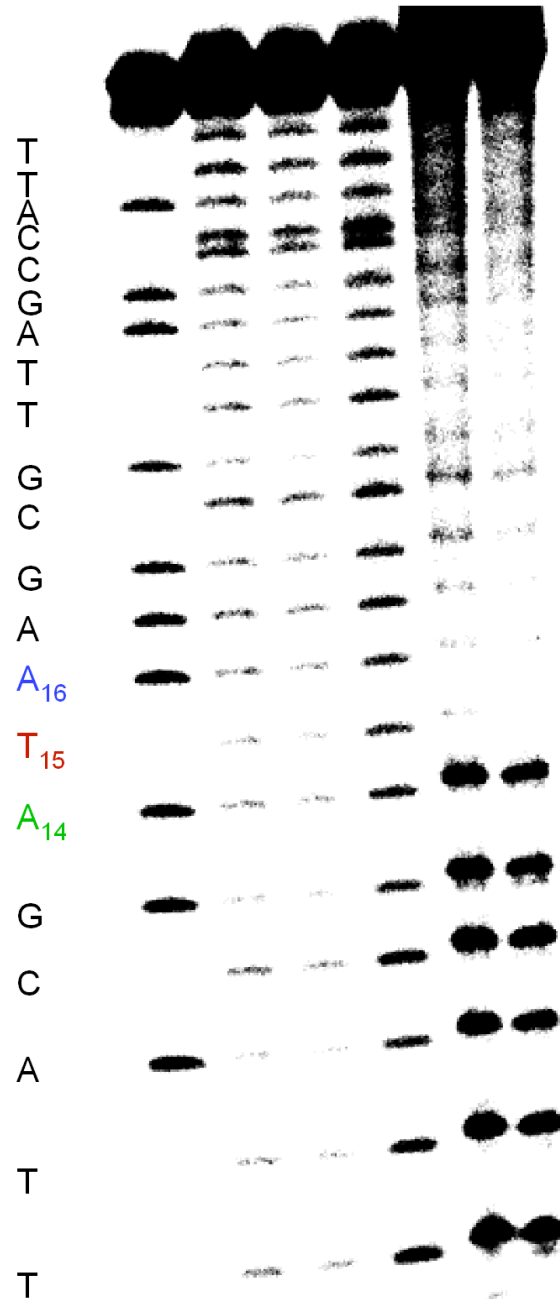
Time (min): 0.5 1 1 2 3
 Lane: 1 2 3 4 5 6



Supporting Information Figure 30. Hydroxyl radical cleavage of **3j**. **2j** (lanes 2-4) and **3j** (lanes 5-6) were treated with OH• for the indicated time. Lane 1; G/A sequencing of **2j**.

3k 5'-d(DOB T₄₇C GTA ATG CAG TCT)
 3'-d(ATT ACC GAT TGC GAA₁₆ T₁₅ A₁₄G CAT TAC GTC AGA)

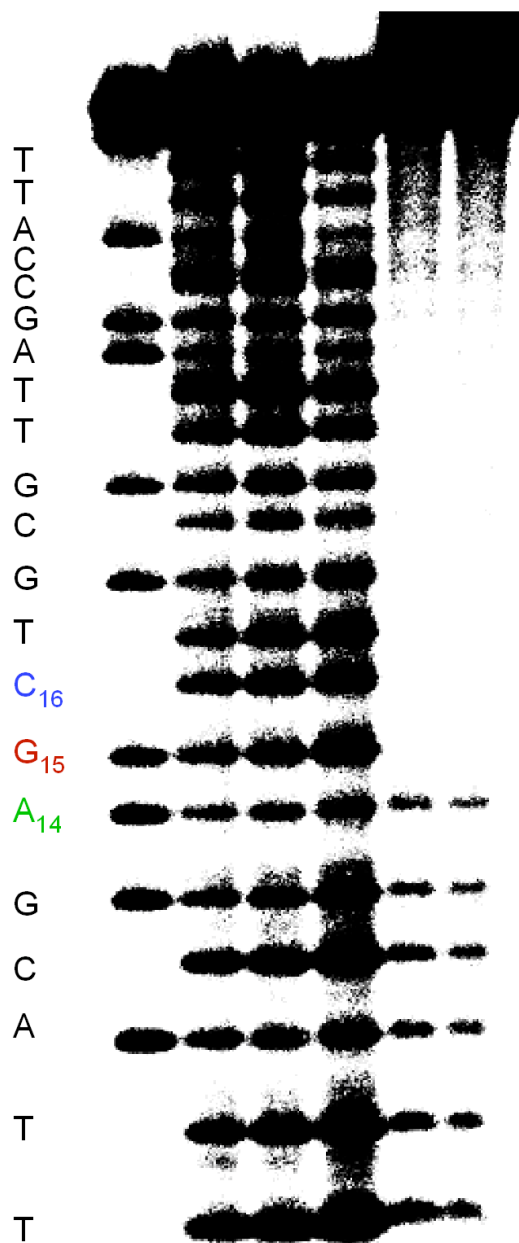
Time (min): 0.5 1 1 2 3
 Lane: 1 2 3 4 5 6



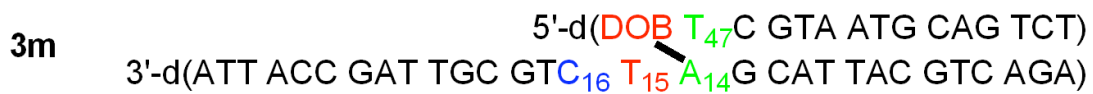
Supporting Information Figure 31. Hydroxyl radical cleavage of **3k**. **2k** (lanes 2-4) and **3k** (lanes 5-6) were treated with OH• for the indicated time. Lane 1; G/A sequencing of **2k**.

31 5'-d(DOB T₄₇C GTA ATG CAG TCT)
 3'-d(ATT ACC GAT TGC GTC₁₆ G₁₅ A₁₄G CAT TAC GTC AGA)

Time (min): 0.5 1 1 2 3
 Lane: 1 2 3 4 5 6

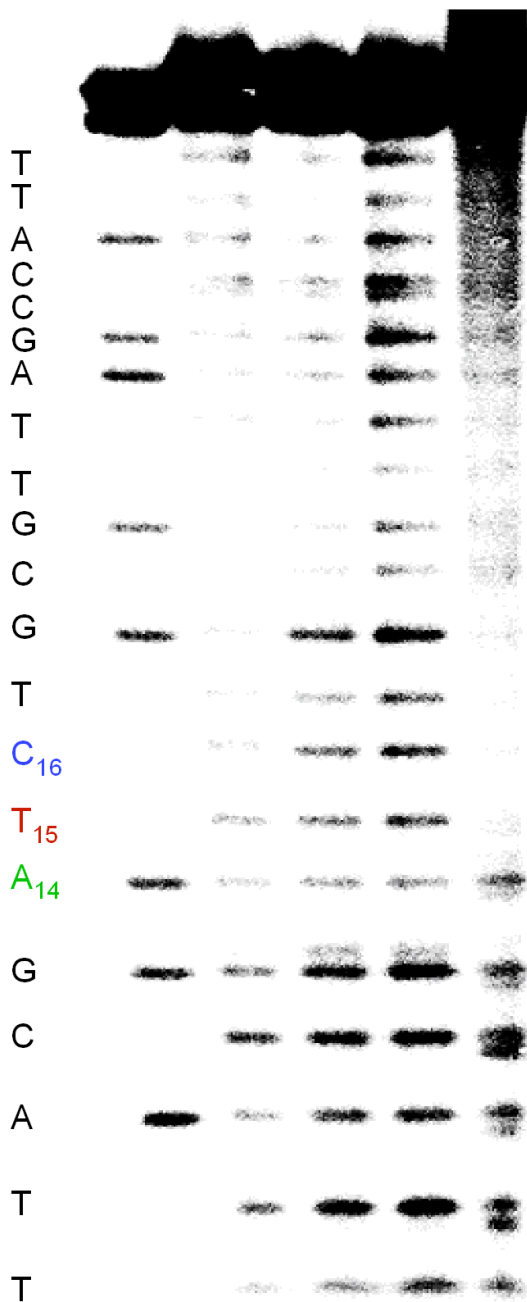


Supporting Information Figure 32. Hydroxyl radical cleavage of **31**. **21** (lanes 2-4) and **31** (lanes 5-6) were treated with OH• for the indicated time. Lane 1; G/A sequencing of **21**.



Time (min): 0.5 1 1 2

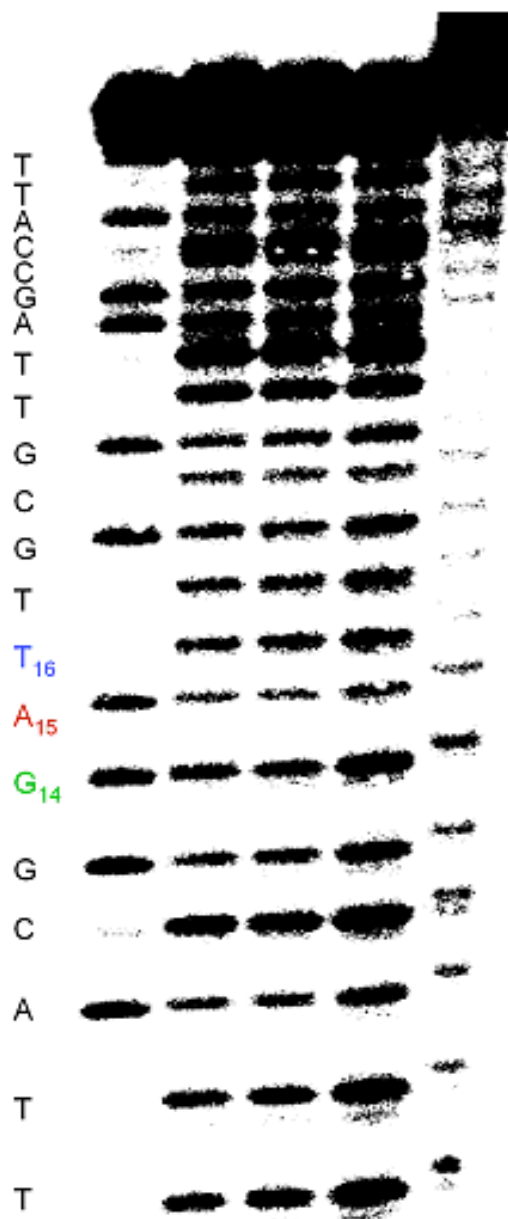
Lane: 1 2 3 4 5



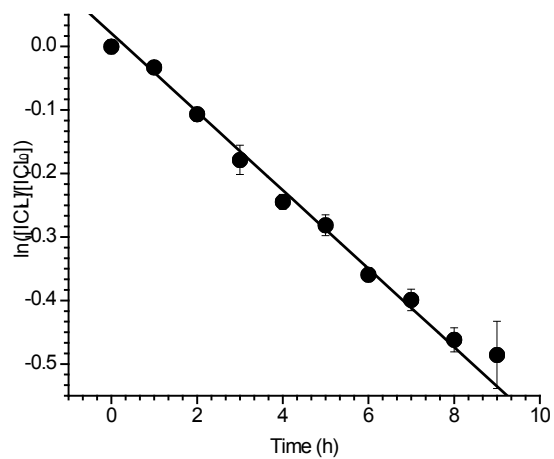
Supporting Information Figure 33. Hydroxyl radical cleavage of **3m**. **2m** (lanes 2-4) and **3m** (lane 5) were treated with OH• for the indicated time. Lane 1; G/A sequencing of **2m**.

3p 5'-d(DOB C₄₇ C GTA ATG CAG TCT)
 3'-d(ATT ACC GAT TGC GTT₁₆ A₁₅ G₁₄ G CAT TAC GTC AGA)

Time (min): 0.5 1 1 2
 Lane: 1 2 3 4 5

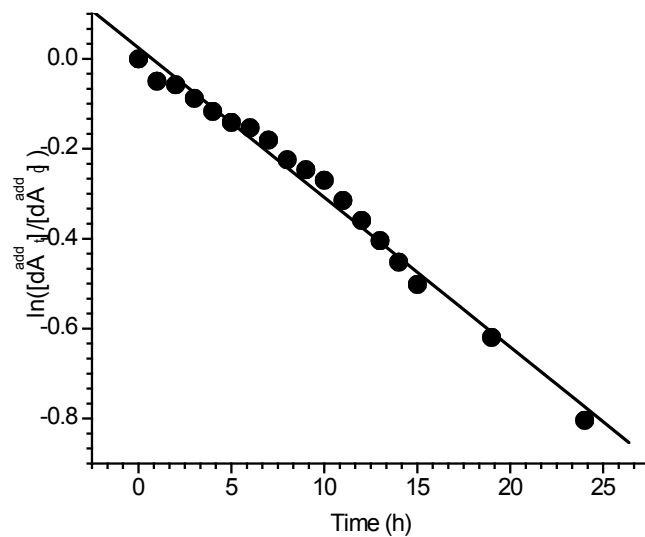


Supporting Information Figure 34. Hydroxyl radical cleavage of **3p**. **2p** (lanes 2-4) and **3p** (lane 5) were treated with OH• for the indicated time. Lane 1; G/A sequencing of **2p**.

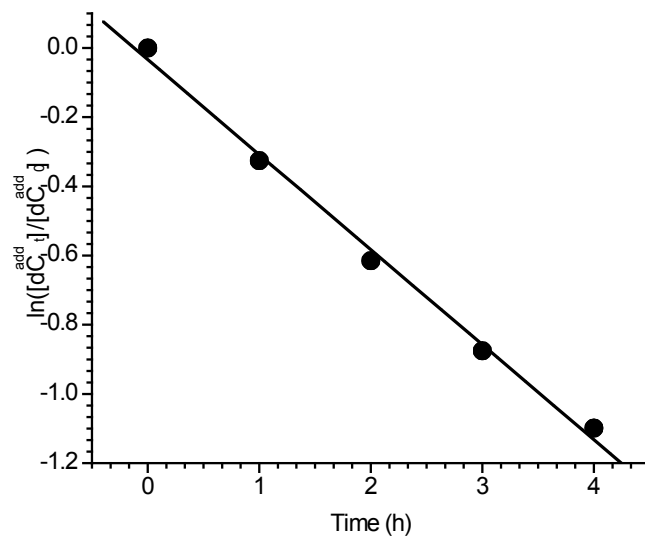


Supporting Information Figure 35. Plot of ICL **3i** decomposition as a function of time.

A.



B.



Supporting Information Figure 36. Kinetic plot of 1,4-butanedial adduct decomposition. A) dA adduct. B) dC adduct.